Juvenile myelomonocytic leukemia with t(7;11)(p15;p15) and *NUP98-HOXA11* fusion

Yoko Mizoguchi,[1,2]* Naoto Fujita,[1] Tomohiko Taki,[3] Yasuhide Hayashi,[4] and Kazuko Hamamoto[1]

The t(7;11)(p15;p15) translocation has been reported as a rare and recurrent chromosomal abnormality in acute myeloid leukemia (AML) patients. The *NUP98-HOXA9* fusion gene with t(7;11)(p15;p15) was identified and revealed to be essential for leukemogenesis and myeloproliferative disease. To date, t(7;11)(p15;p15) with *NUP98-HOXA11* fusion has been reported only in one case of ph-negative chronic myeloid leukemia (CML). Here, we report a case of a 3-year-old girl with juvenile myelomonocytic leukemia (JMML) carrying t(7;11)(p15;p15) abnormality with *NUP98-HOXA11* fusion. AML chemotherapy followed by bone marrow transplantation (BMT) was found to be effective in treating this disorder, and she remains in complete remission for 3 years after BMT. We suggest the possibility that AML chemotherapy might be effective for treating JMML with t(7;11)(p15;p15) abnormality and *NUP98-HOXA11* fusion. Am. J. Hematol. 00:000–000, 2009. © 2009 Wiley-Liss, Inc.

Introduction

Juvenile myelomonocytic leukemia (JMML) is refractory to chemotherapy, and the only curative treatment is hematopoietic stem cell transplantation (HSCT). Although the 5-year probability of event-free survival (EFS) in JMML patients receiving HSCT is approximately 50%, relapse remains the major form of treatment failure and is observed in up to 50% patients [1]. Thus far, somatic mutation in *PTPN11, RAS, or NF1* and monosomy 7 are known to be the essential chromosomal or genetic abnormalities in JMML. The t(7;11)(p15;p15) translocation is reported as a rare and recurrent chromosomal abnormality detected mainly in acute myeloid leukemia (AML) patients [2–5]. *NUP98-HOXA9* fusion involving t(7;11)(p15;p15) was first reported by both Nakamura et al. [6] and Borrow et al. [7]; subsequently, this abnormal fusion has been shown to be critical for leukemogenesis and preleukemic phase [8,9]. In this paper, we report a case of JMML involving t(7;11)(p15;p15) abnormality with *NUP98-HOXA11* fusion. *NUP98-HOXA11* fusion has been reported only in a ph-negative chronic myeloid leukemia (CML) patient [10], and this previous case and our present case indicate that *NUP98-HOXA11* fusion might also be related closely to leukemogenesis and preleukemic phase.

Case Report

A 3-year-old Japanese girl who presented with wheezing was referred to our hospital because of leukocytosis and anemia. Her family history revealed that her grandmother had died of myelodysplastic syndrome (MDS). A physical examination revealed hepatosplenomegaly, but skin eruptions or lymph node swellings were not detected. She had no clinical evidence of autoimmune lymphoproliferative syndrome, neurofibromatosis Type 1, Noonan syndrome, Costello syndrome, or any cardiofaciocutaneous syndromes with germline RAS-pathway mutation. Laboratory data at the time of presentation were as follows: hemoglobin (Hb), 8.2 g/dl; platelets, 165,000/μl; white blood cells, 39,400/μl with 8% monocytoid cells, 13% myelocytes, 8% metamyelocytes, and 1.5% blast cells. Biochemical tests showed normal level of HbF (2%) and low level of neutrophil alkaline phosphatase (score, 150). The serum lysozyme level was elevated (56.8 μl/ml). Infections such as those caused by cytomegalovirus, Epstein-Barr virus, and human herpes virus Type 6 were excluded. Bone marrow aspirate revealed hypercellular marrow with 1% blast cells, and a bilineage myelodysplasia such as macroerythroblasts, Pseudo-Perger-Hüet anomaly, and chromatin clumping in neutrophils were found. Chromosome analysis of the bone marrow showed 46,XX,t(7;11)(p15;p15) in all 20 cells analyzed. Spontaneous growth and hypersensitivity to the granulocyte/macrophage colony-stimulating factor (GM-CSF) were observed in the colony assay. A heterozygous mutation of *NRAS* gene (38G>A, G13D), but not *KRAS*, *HRAS*, or *PTPN11*, was also observed in leukemic cells of the patient. These findings were consistent with the diagnosis of JMML in accordance with the diagnostic criteria of JMML established by the European Working Group of MDS in Childhood [1].

After a 3-week observation period without therapy, her WBC count was 57,600/μl, including 10.5% blast cells; Hb level, 7.2 g/dl; and platelet count, 83,000/μl. Bone marrow pictures revealed hyperplastic cellularity with 3% blast cells. Because of the increasing ratio of blast cells, which were similar to myelocytes, in peripheral blood (PB) and the chromosomal abnormality, which is mainly observed in AML, she was treated with induction chemotherapy (cytarabine, etoposide, and mitoxantrone) on the Japanese Childhood AML Cooperative Study Group Protocol, AML 99 [11]. She achieved complete remission after induction therapy, and the t(7;11)(p15;p15) abnormality disappeared. After two additional courses of intensive chemotherapy (high-dose cytarabine, etoposide, idarubicin and mitoxantrone),

[1]Department of Pediatrics, Hiroshima Red Cross Hospital and Atomic Bomb Survivors Hospital, Hiroshima, Japan; [2]Department of Pediatrics, Hiroshima University Hospital, Hiroshima, Japan; [3]Department of Molecular Laboratory Medicine, Kyoto Prefectural University of Medicine, Graduate School of Medical Science, Kyoto, Japan; [4]Department of Hematology/Oncology, Gunma Children's Medical Center, Gunma, Japan

Conflict of interest: Nothing to report.

*Correspondence to: Yoko Mizoguchi, Department of Pediatrics, Hiroshima University Hospital, 1-2-3 Kasumi, Minami-ku, Hiroshima 734-8551, Japan. E-mail: yoyotti129@yahoo.co.jp

Received for publication 22 October 2008; Revised 24 January 2009; Accepted 26 January 2009

Am. J. Hematol. 00:000–000, 2009.

Published online in Wiley InterScience (www.interscience.wiley.com).
DOI: 10.1002/ajh.21373

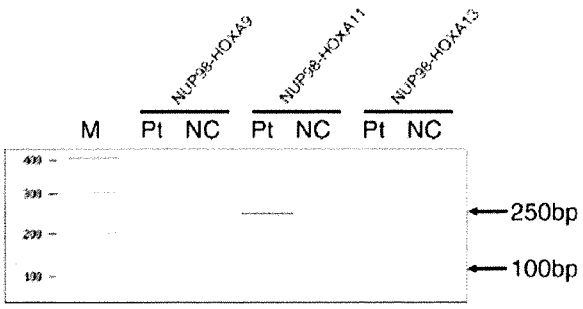

Figure 1. Detection of the NUP98-HOXA11 fusion transcript in the JMML patient by RT-PCR. M, size marker; Pt, patient; NC, normal negative control. The primers used for detection were as follows: NUP98-11S1 and HOXA9-1AS, *NUP98-HOXA9*; NUP98-11S1 and HOXA11-1AS, *NUP98-HOXA11*; and NUP98-11S1 and HOXA13-1AS, *NUP98-HOXA13*.

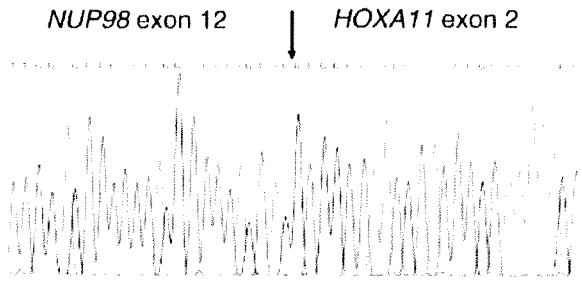

Figure 2. Direct sequencing of the NUP98-HOXA11 fusion transcript junction. Arrow indicates the fusion point. [Color figure can be viewed in the online issue, which is available at www.interscience.wiley.com.]

she received allogeneic HSCT from a human leukocyte antigen (HLA)-identical sibling donor. The conditioning regimen consisted of total body irradiation (TBI, 6 Gy in 3 fractions over 2 d), fludarabin (35 mg/(m^2 day) for 4 d), melphalan (70 mg/(m^2 day) for 2 d), and cytarabine (3 mg/(m^2 day) for 4 d) combined with the granulocyte colony-stimulating factor (G-CSF). A graft-versus-host disease (GVHD) prophylaxis consisted of a short course of methotrexate alone. A sustained recovery of neutrophils was achieved on day 30. without any severe complications. She developed Grade I acute GVHD of the skin on day 56 and mild chronic GVHD of the skin on day 180; both these conditions were improved by administering topical steroids alone. A temporary pulmonary hypertension was also observed on day 120 and was treated with bosentan. She remains in complete remission for about 3 years after bone marrow transplant (BMT).

Results

To isolate the fusion partner of *NUP98*, we performed reverse transcription (RT)-PCR using antisense primers based on *HOXA9*, *HOXA11*, and *HOXA13* and detected a band of approximately 250 bp and a very faint band of approximately 100 bp when the primers NUP98-11S1 and HOXA11-1AS were used (see Fig. 1). Direct sequence analysis showed that the RT-PCR product was an in-frame fusion transcript of *NUP98-HOXA11* containing exon 12 of the *NUP98* gene fused to exon 2 of the *HOXA11* gene (see Fig. 2).

Discussion

The t(7;11)(p15;p15) translocation with *NUP98-HOXA11* fusion was first reported in a patient with ph-negative CML [10], and our present case is the second case of carrying t(7;11)(p15;p15) aberration with the *NUP98-HOXA11* gene fusion. The t(7;11)(p15;p15) translocation is known as an uncommon and recurrent chromosomal abnormality mainly associated with AML [2–4]. Most cases of this abnormality are observed in the Oriental population, especially in Japanese patients [2]. Thus far, the t(7;11) abnormality with the *NUP98-HOXA9* gene fusion has been reported in AML, MDS, and chronic myelomonocytic leukemia (CMML) patients [3–5], and this abnormal fusion was found to induce a preleukemic phase in a mouse model [8,9]. Iwasaki et al. [9] indicated that approximately 20% of the transgenic mice in which the chimeric *NUP98-HOXA9* fusion cDNA was expressed in promyelocytes progressed to AML after a long latent period, whereas nonleukemic transgenic mice showed an increased G-CSF response and a high self-renewal capacity of myeloid progenitors as compared with wild-type mouse. In our JMML case, hypersensitivity to GM-CSF and spontaneous growth in the colony assay were observed. In addition, it was reported that other factors were required for complete leukemogenesis in *NUP98-HOX* fusion [12,13]. For example, *Meis1* coexpression dramatically induced the development of AML having *NUP98-HOXD13* with a short latency [12]. Slape. C et al. also reported that no *NRAS* or *KRAS* mutations were identified in 12 *NUP98-HOXD13* mice with MDS, whereas three *NRAS* and four *KRAS* mutations were identified in *NUP98-HOXD13* mice with acute nonlymphocytic leukemia (ANLL) and they suggested that the *RAS* mutations occurred as leukemia progression events [13]. These findings suggested that *NUP98-HOX* gene fusion is relevant to preleukemic phase, and it requires additional cofactors for complete leukemogenesis. On the other hand, oncogenic point mutations of *RAS* gene are also found in 20% of JMML patients [14]. In our case, we considered that both *NUP98-HOXA11* fusion and a point mutation of *NRAS* gene were associated with the development of myeloproliferative disorder (MPD), however, the relationship between *NUP98-HOXA11* fusion and a mutation of *NRAS* gene is uncertain.

JMML is a clonal myeloproliferative disorder of early childhood. JMML is defined to possess features of both MDS and MPD, and it is classified into MDS/MPD with ph-negative CML and CMML in the WHO classification [15]. Generally, chemotherapy regimen for AML is thought to be ineffective for JMML, and BMT has been proposed as the only treatment of choice. In our case, we found an increased ratio of blast cells, which were similar to myelocytes, in PB within a short period and chromosomal abnormality of t(7;11)(p15;p15). On the basis of clinical features, we thought this case had a feature of AML and administered AML chemotherapy to the patient, followed by HSCT; the patient achieved complete remission by this treatment strategy. The first reported case of t(7;11)(p15;p15) with *NUP98-HOXA11* gene fusion was a patient with ph-negative CML [10], who developed an acute leukemia phase within a short period and achieved complete remission after treatment with idarubicin and cytarabine, which are used for treating AML. Furthermore, in our case, AML chemotherapy followed by HSCT proved to be effective for treating the disorder. Thus, these two cases indicate that AML chemotherapy may be effective for treating leukemia or MPD with *NUP98-HOXA11* gene fusion.

Materials and Methods

RNA extraction and reverse transcription-polymerase chain reaction analysis. Total RNA was extracted from the bone marrow mononuclear cells at the onset by using the Isogen LS Kit (Wako Nippon Gene,

Osaka, Japan). Four micrograms of total RNA was reverse transcribed to cDNA in a total volume of 33 μl with a random hexamer primer by using the Ready-To-Go You-Prime First-Strand Beads (GE Healthcare, Buckinghamshire, England). Polymerase chain reaction (PCR) was performed with AmpliTaq Gold DNA polymerase (Applied Biosystems, Tokyo, Japan) by using the reagents recommended by the manufacturer. The primers used were as follows: NUP98-11S1, AGCACCTGG GACTCTTGGAA; HOXA9-1AS, CATTTTCATCCTGCGGTTCTG; HOX A11-1AS, CTCTCGGATCTGGTACTTGGT; HOXA13-1AS, CCT CCTA-TAGGA GCTGGCAT. After 35 rounds of PCR (30 s at 94°C, 30 s at 55°C, 1 min at 72°C), the detection of PCR products was performed with the Agilent 2100 Bioanalyzer and the DNA 1000 Lab Chip kit as described previously [16].

References

1. Clinical Trial Protocol EWOG-MDS (The European Working Group of MDS in Childhood) 2006 Final version [internet]: November 30, 2006. Available from http://www.ewog-mds.org.
2. Huang SY, Tang JL, Liang YJ, et al. Clinical, haematological and molecular studies in patients with chromosome translocation t(7;11): A study of four Chinese patients in Taiwan. Br J Haematol 1997;96:682–687.
3. Wong KF, So CC, Kwong YL. Chronic myelomonocytic leukemia with t(7;11)(p15;p15) and *NUP98/HOXA9* fusion. Cancer Genet Cytogenet 1999; 115:70–72.
4. Hatano Y, Miura I, Nakamura T, et al. Molecular heterogeneity of the *NUP98/HOXA9* fusion transcript in myelodysplastic syndrome associated with t(7;11)(p15;p15). Br J Haematol 1999;107:600–604.
5. Romana SP, Radford-Weiss I, Abdelali RB, et al. & on behalf of the Groupe Francophone de Cytogénétique Hématologique (GFCH). NUP98 rearrangements in hematopoietic malignancies: A study of the Groupe Francophone de Cytogénétique Hématologique. Leukemia 2006;20:696–706.
6. Nakamura T, Largaespada DA, Lee MP, et al. Fusion of the nucleoporin gene *NUP98* to *HOXA9* by the chromosome translocation t(7;11)(p15;p15) in human myeloid leukemia. Nat Genet 1996;12:154–158.
7. Borrow J, Shearman AM, Stanton VP, et al. The t(7;11)(p15;p15) translocation in acute myeloid leukemia fuses the genes for nucleoporin *NUP98* and class I homeoprotein *HOXA9*. Nat Genet 1996;12:159–167.
8. Kroon E, Thorsteinsdottir U, Mayotte N, et al. NUP98-HOXA9 expression in hemopoietic stem cells induces chronic and acute myeloid leukemias in mice. EMBO J 2001;20:350–361.
9. Iwasaki M, Kuwata T, Yamazaki Y, et al. Identification of cooperative genes for *NUP98-HOXA9* in myeloid leukemogenesis using a mouse model. Blood 2005;105:784–793.
10. Suzuki A, Ito Y, Sashida G, et al. t(7;11)(p15;p15) chronic myeloid leukaemia developed into blastic transformation showing a novel *NUP98/HOXA11* fusion. Br J Haematol 2002;116:170–172.
11. Shimada A, Taki T, Tabuchi K, et al. *KIT* mutations, and not *FLT3* internal tandemduplication, are strongly associated with a poor prognosis in pediatric acute myeloid leukemia with t(8;21):A study of the Japanese Childhood AML Cooperative Study Group. Blood 2006;107:1806–1809.
12. Pineault N, Buske C, Feuring-Buske M, et al. Induction of acute myeloid leukemia in mice by the human leukemia-specific fusion gene *NUP98-HOXD13* in concert with *Meis1*. Blood 2003;101:4529–4538.
13. Slape C, Liu LY, Beachy S, et al. Leukemic transformation in mice expressing a *NUP98-HOXD13* transgene is accompanied by spontaneous mutations in *Nras*, *Kras*, and *Cbl*. Blood 2008;112:2017–2019.
14. Koike K, Matsuda K. Recent advances in the pathogenesis and management of juvenile myelomonocytic leukaemia. Br J Haematol 2008;141:567–575.
15. Swerdlow SH, Campo E, Harris NL, et al. WHO Classification of Tumors of Haematopoietic and Lymphoid issues. Lyon: IRAC Press; 2008. pp 104–107.
16. Gottwald E, Muller O, Polten A. Semiquantitative reverse transcription-polymerase chain reaction with the Agilent 2100 Bioanalyzer. Electrophoresis 2001; 22:4016–4022.

Single nucleotide polymorphism genomic arrays analysis of t(8;21) acute myeloid leukemia cells

Tadayuki Akagi,[1] Lee-Yung Shih,[2,3] Seishi Ogawa,[4,5] Joachim Gerss,[6] Stephen R. Moore,[7] Rhona Schreck,[7] Norihiko Kawamata,[1] Der-Cherng Liang,[8] Masashi Sanada,[4,5] Yasuhito Nannya,[4] Stefan Deneberg,[1] Vasilios Zachariadis,[10] Ann Nordgren,[10] Jee Hoon Song,[1] Martin Dugas,[6] Sören Lehmann,[1,9] and H. Phillip Koeffler[1]

[1]Division of Hematology and Oncology, Cedars-Sinai Medical Center, UCLA School of Medicine, Los Angeles, CA, USA; [2]Division of Hematology-Oncology, Chang Gung Memorial Hospital, Taipei, Taiwan; [3]School of Medicine, Chang Gung University, Taoyuan, Taiwan; [4]Department of Hematology and Oncology and [5]the 21st century COE program, Graduate School of Medicine, University of Tokyo, Tokyo, Japan; [6]Department of Medical Informatics and Biomathematics, University of Munster, Munster, Germany; [7]Pathology/Laboratory Medicine and Medical Genetics Institute, Cedars-Sinai Medical Center, Los Angeles, CA, USA; [8]Department of Pediatrics, Mackay Memorial Hospital, Taipei, Taiwan; [9]Department of Hematology, and [10]Department of Clinical Genetics, Karolinska University Hospital, Stockholm, Sweden

ABSTRACT

Translocation of chromosomes 8 and 21, t(8;21), resulting in the *AML1-ETO* fusion gene, is associated with acute myeloid leukemia. We searched for additional genomic abnormalities in this acute myeloid leukemia subtype by performing single nucleotide polymorphism genomic arrays (SNP-chip) analysis on 48 newly diagnosed cases. Thirty-two patients (67%) had a normal genome by SNP-chip analysis (Group A), and 16 patients (33%) had one or more genomic abnormalities including copy number changes or copy number neutral loss of heterozygosity (Group B). Two samples had copy number neutral loss of heterozygosity on chromosome 6p including the *PIM1* gene; and one of these cases had E135K mutation of Pim1. Interestingly, 38% of Group B and only 13% of Group A samples had a *KIT*-D816 mutation, suggesting that genomic alterations are often associated with a *KIT*-D816 mutation. Importantly, prognostic analysis revealed that overall survival and event-free survival of individuals in Group B were significantly worse than those in Group A.

Key words: t(8;21), *AML1-ETO*, CNN-LOH, SNP-chip, *KIT*, *PIM1*.

Citation: Akagi T, Shih L-Y, Ogawa S, Gerss J, Moore SR, Schreck R, Kawamata N, Liang D-C, Sanada M, Nannya Y, Deneberg S, Zachariadis V, Nordgren A, Song JH, Dugas M, Lehmann S, and Koeffler HP. Single nucleotide polymorphism genomic arrays analysis of t(8;21) acute myeloid leukemia cells. Haematologica 2009;94:1301-1306. doi:10.3324/haematol.2009.005744

Introduction

The t(8;21)(q22;q22) translocation occurs in 40% of patients with acute myeloid leukemia (AML) of the FAB-M2 subtype, and constitutes 12% of all newly diagnosed cases of AML. This translocation leads to a fusion product of AML1 (also called RUNX1 or CBFβ) and ETO (also called MTG8). Data have suggested that the translocation is an early event in leukemogenesis.[1] Furthermore, the t(8;21) translocation can be found in neonatal Guthrie blood spots of infants that later developed *AML1-ETO* leukemia, suggesting that the translocation can precede development of AML by up to ten years.[2,3]

Several murine models have demonstrated that *AML1-ETO* alone is not sufficient to induce leukemia. Murine bone marrow cells expressing tetracycline-inducible *AML1-ETO* transgene did not develop leukemia:[4] but developed myeloproliferative disorders.[5] In contrast, 30-55% of *AML1-ETO*-expressing mice treated with the DNA-alkylating mutagen N-ethyl-N-nitrosourea (ENU) developed AML.[6,7] These findings strongly suggest that a secondary hit is necessary for the development of t(8;21) AML.

The protooncogene *KIT* is a receptor tyrosine kinase. Activating mutations of *KIT* including those in either the extracellular (exon 8) region or the protein kinase domains

Acknowledgments: we thank members of our laboratories for helpful discussions. Funding: this work was supported by NIH grants, Parker Hughes Fund (HPK); and the grant support of NHRI-EX96-9434SI (LS) and MMH-E-96009 (DL). HPK is the holder of the Mark Goodson endowed Chair in Oncology Research and is a member of the Jonsson Cancer Center and the Molecular Biology Institute, UCLA. MD is supported by the European Leukemia Network (funded by the 6th Framework Program of the European Community). This article is dedicated to the memory of David Golde, a mentor and friend. Manuscript received on January 7, 2009. Revised version on arrived March 11, 2009. Manuscript accepted on March 25, 2009.
Correspondence: Tadayuki Akagi, Department of Stem Cell Biology, Graduate School of Medical Science, Kanazawa University, 13-1 Takara-machi, Kanazawa, Ishikawa 920-8640, Japan. E-mail: tadayuki@staff.kanazawa-u.ac.jp. Sören Lehmann, Department of Hematology M54, Karolinska University Hospital, Huddinge, Stockholm 141 86, Sweden. E-mail: soren.lehmann@ki.se.
The online version of this article contains a supplementary appendix.

(D816 mutation) are found in 2% and 11% of t(8;21) AML samples, respectively.[8,9] FLT3 is also a receptor tyrosine kinase. Two frequent activating mutations of *FLT3*, FLT3-internal tandem duplication (ITD) and FLT3-tyrosine kinase domain (TKD) mutation, are detected in a range of 2-8% and 2-4% of samples of t(8;21) AML, respectively.[10,11] Mutation of *NRAS* at either codon 12, 13 or 61 is found in 9% of t(8;21) AML samples.[10,11]

High-density single nucleotide polymorphism genomic arrays (SNP-chip) allow the detection of copy number changes, as well as copy number neutral loss of heterozygosity (CNN-LOH) in leukemia samples.[12-18] In order to screen for secondary alteration(s) that potentially could cause *AML1-ETO* transformed cells to develop acute myeloid leukemia, we performed SNP-chip analysis of 48 t(8;21) AML samples. The use of CNAG (copy number analysis for Affymetrix GeneChips) program[12] and an algorithm AsCNAR (allele-specific copy number analysis using anonymous references)[18] allows identification of hidden abnormalities and novel disease-related genomic regions in the leukemia samples. Here, we found that genomic changes detected by SNP-chip analysis are associated with a poor overall and event-free survival in t(8;21) AML.

Design and Methods

Patient samples, determination of mutant genes and statistical analysis

Genomic DNA of 48 anonymized samples of t(8;21) AML cells were obtained from Chang-Gung Memorial Hospital, Chang-Gung University in Taiwan after obtaining informed consent. These samples had been frozen over a span of 14 years (July 1990 to July 2004). Sample information is shown in the *Online Supplementary Table S1*. The study has been approved by Cedars-Sinai Medical Center (IRB number 4485).

To detect an AML1-ETO fusion transcript, RT-PCR was performed using specific primers as described previously.[19] Mutation analysis of the *KIT* gene for the t(8;21) AML samples was reported previously.[20] Statistical analysis is described in the *Online Supplementary Design and Methods section.*

SNP-chip analysis

Genomic DNA isolated from t(8;21) AML cells was subjected to GeneChip Human mapping microarray (SNP-chip, Affymetrix, Santa Clara, CA, USA) as described previously;[12,13] ten samples (cases #47, #51, #52, #54, #56, #57, #59, #60, #61 and #62) were examined with the 250 K array, and the other 38 samples were analyzed with the 50 K array. The allele-specific copy numbers (AsCNs) were estimated using normal genomic DNA from peripheral blood of normal volunteers as controls.[13] The array does not contain Y-chromosome probes; therefore, we summarize the SNP-chip data without sex chromosomes. Size, position and location of genes were identified with UCSC Genome Browser (*http://genome.ucsc.edu/*). Copy number changes previously described as copy number variants (*http://projects.tcag.ca/variation/*) were excluded.

Fluorescence in situ hybridization (FISH) analysis

Interphase hybridizations were performed following the manufacturer's instructions and standard protocols. Probes for the *SNRPN* gene, 15q telomere, 7p telomere and 7q telomere were obtained from Cytocell (Cambridge, United Kingdom); and probes for the *MYC* gene as well as the centromere of chromosome 8 were purchased from Abbott Molecular (Abbott Park, IL, USA). Fifty interphase cells were scored for each sample, with 20 cells scored in controls (bone marrow controls with normal karyotypes). Signal patterns were normal for all controls with all probe sets.

Analysis of the PIM1 gene

Six coding exons of the *PIM1* gene were amplified using specific primers from genomic DNA of cases #39 and #41. After purification of the PCR products from agarose gel, nucleotide sequences were determined. Primer sequences will be provided upon request. These 6 exons of other t(8;21) AML samples were examined by single strand conformation polymorphism (SSCP) as described in the *Online Supplementary Design and Methods* section.

To determine the frequency of missense mutations of the *PIM1* gene within exon 4, this region of 34 t(8;21) AML samples and 40 normal blood DNA samples were amplified by PCR using specific primer (5'-TCC TGG AGA GGC CCG AGC-3' and 5'-TTG AGG TCG ATA AGG ATG-3'). The PCR product (178 bp) was treated with a restriction enzyme Hpy188III for 1h. PCR products from wild-type allele are not digested but mutated allele are digested by the restriction enzyme.

Results and Discussion

SNP-chip analysis of 48 t(8;21) acute myeloid leukemia samples

SNP-chip analysis of 48 t(8;21) acute myeloid leukemia (AML) samples revealed several genomic copy number changes, as well as copy number neutral loss of heterozygosity (CNN-LOH). As shown in Table 1 and *Online Supplementary Figure S1*, 32 patients (67%) had a normal genome by SNP-chip analysis (Group A, mean age is 23, range 2-74). In contrast, 16 patients (33%) had one or more genomic abnormalities (Group B, mean age is 31, range 4-61). Thus, these copy number changes probably harbor dysregulated leukemia-associated genes in t(8;21) AML. Cytogenetics showed that case #33 had trisomy 4 in 2 out of 15 cells (13%), and case #34 had monosomy 18 in 6 out of 24 cells (25%) (*Online Supplementary Table S1*). These minor clones were not detected by SNP-chip analysis. Case #40 had tetraploidy in 23 out of 25 cells; 2-fold gene-dosage in all chromosomes was masked and detected as normal gene-dosage.

Next, we compared SNP-chip results and gene mutations. Ten out of 48 samples (18%) had a *KIT*-D816 mutation. Interestingly, 6 (case #7, #14, #26, #37, #40, and #52) of the 10 samples were found in Group B,

Table 1. Chromosomal regions with copy number changes and copy number neutral loss of heterozygosity in t(8; 21) acute myeloid leukemia samples.

Case #	Status	Location	Physical localization: Proximal	Distal	Size (Mb)	Genes
6	Dup	8q24.23	137,858,383	137,892,295	0.03	No known genes
7	Dup	18q21.32	56,209,691	56,315,439	0.1	No known genes
	CNN-LOH	11pter-p12	1,938,894	42,449,197	40.5	>10 genes including *CDKN1C*, *HRAS*, and *WT1*
13	Tri	Trisomy 15	–	–	–	>10 genes
14	Del	7q35-q36.1	146,128,574	148,288,861	2.1	*CNTNAP2*, *CUL1*, *EZH2*, *PDIA4*, *ZNF425*, *ZNF298*
17	Del	9q13-q36.1	68,275,512	84,477,002	16.2	>10 genes
26	Tri	Trisomy 4	–	–	–	>10 genes including *KIT*
	Del	13q21.1	54,339,313	54,457,753	0.1	no known genes
28	Dup	15q21.1-qter.	46,526,374	100,182,183	53.7	>10 genes
	Del	16pter -p13.2	1,543,577	7,010,644	5.5	>10 genes
34	Del	7q31.2-qter.	116,548,736	158,554,645	42	>10 genes
	Dup	8q22.1-qter.	97,255,867	143,902,698	46.6	>10 genes including *MYC*
	Del	9q33.1	116,515,445	117,926,188	1.4	*TNFSF15*, *TNFSF8*, *TNC*, *DEC1*, *CTS9*, *EST-YD1*
	Del	9q13-q31.3	68,275,512	109,232,711	41	> 10 genes
37	Dup	4p16.1-q28.3	7,902,265	139,029,890	131.1	>10 genes including *KIT*
	Dup	8q22.1-qter.	96,550,847	143,902,698	47.4	>10 genes including *MYC*
39	Tri	Trisomy 4	–	–	–	>10 genes including *KIT*
	Dup	14q11.2-q13.1	19,285,288	33,978,199	14.7	>10 genes
	CNN-LOH	6pter-p12.3	150,610	46,902,007	46.8	>10 genes including *PIM1* and *CDKN1A*
40	Mono	Monosomy 11	–	–	–	>10 genes
41	CNN-LOH	6p-ter. - 6p21.1	150,610	44,873,513	44.7	>10 genes including *PIM1* and *CDKN1A*
43	Mono	Monosomy 7	–	–	–	>10 genes
52	Dup	5q14.1	77034347	77551493	0.5	*TBCA*, *AP3B1*
59	CNN-LOH	11q13.2 - q-ter.	67259252	134439182	67.2	>10 genes
	Del	16q21	57560512	58960978	1.4	no known genes
60	Dup	1q41 - q-ter.	211518337	245353397	33.8	>10 genes
	Del	7q31.32	121860398	122756128	0.9	*CADPS2*, *RNF133*, *RNF148*, *AK058116*, *TAS2R16*, *SLC13A1*
	Del	7q31.33 - q-ter.	123544140	158605053	35.1	>10 genes

Physical localization and size (Mb) are obtained from UCSC Genome Browser. Copy number changes previously described as copy number variant were excluded. CNN-LOH; copy number neutral loss of heterozygosity, Del; deletion, Dup; duplication, Tri; trisomy, Mono; monosomy, ter.; terminal.

demonstrating that *KIT*-D816 mutation is significantly associated with Group B ($p<0.05$, χ^2 test). This result suggests that copy number changes are often involved in cases with a *KIT*-D816 mutation in t(8;21) AML.

Recurrent copy number changes in t(8;21) acute myeloid leukemia samples

Two cases (#34 and #37) had a duplication on chromosome 8 from 8q22.1 to q-terminal including the *MYC* gene; and 2 cases (#13 and #28) had a trisomy/duplication on chromosome 15 with common duplicated region at 15q21.1-15q-terminal (53.7 Mb). Four cases (#14, #34, #43 and #60) had a deletion/monosomy on chromosome 7 with a common deleted region at 7q35 - 7q36.1 (2.1 Mb) including the *CUL1* and *EZH2* genes; and 2 cases (#17 and #34) had a deletion on chromosome 9 with the common deleted region at 9q13 - 9q36.1 (16.2 Mb). Interestingly, a frequent large duplication was found on chromosome 4. Two cases had trisomy 4, and one case had a large region of duplication on chromosome 4 from 4p16.1 to q28.3 (131.1 Mb). All of these amplifications covered the region of the *KIT* gene; and 3 of these cases (#26, #37 and #39) had a *KIT* mutation of either D816Y, D816V or D820G. Amplification of chromosome 4 linked to *KIT* mutations has previously been described in systemic mastocytosis.[21] Thus, the probable increased expression of the mutated form of *KIT* by trisomy 4 or duplication in the region of the gene should give the clone a proliferative advantage.

Validation of copy number change by fluorescence in situ hybridization (FISH)

To validate some of these copy number changes, we used an interphase FISH approach. Case #34 had a duplication of 8q22.1-8q-terminal (46.6 Mb) including the *MYC* gene and a deletion of 7q31.2-7q-terminal (42.0 Mb). The 8q duplication was confirmed using FISH probes for *MYC* and the centromere of chromosome 8 (*Online Supplementary Figure S2A*). In the same case, deletion of chromosome 7q (q31.2 to q-terminal) was confirmed using FISH probes for 7p telomere and

7q telomere (*Online Supplementary Figure S2B*). Case #28 had a large duplication of chromosome 15 (53.7 Mb). The duplication was confirmed using FISH probes for *SNRPN* and 15q telomere (*Online Supplementary Figure S2C*). These results suggest that abnormalities detected by SNP-chip analysis reflected real alterations in AML cells.

Chromosomal regions and candidate genes in genomic areas with copy number neutral loss of heterozygosity (CNN-LOH)

Four cases (8%) had CNN-LOH (Table 1 and *Online Supplementary Figure S1*). Case #7 has CNN-LOH at 11p-terminal-11p12 (40.5 Mb) which included the *CDKN1C*, *HRAS*, *WT1* and *LMO2* genes. Case #39 and #41 have CNN-LOH at 6p-terminal - 6p12.3 (46.8 Mb) and at 6p-terminal - 6p21.1 (44.7 Mb), respectively; and the region contained the *PIM1* and *CDKN1A* genes (Table 1 and *Online Supplementary Figure S3*). Case #59 had CNN-LOH at 11q13.2-q-terminal (67.2 Mb). Raghavan *et al.*[15] showed that approximately 20% AML samples had CNN-LOH, and Gondek *et al.*[16] found that 20% of MDS, 23% of MDS-derived AML, and 35% of MDS/MPD patients had CNN-LOH. In additional studies, we found that 32% of normal karyotype AML samples and 15% of t(15;17) APL samples had CNN-LOH.[17,18] CNN-LOH in t(8;21) AML is less frequent than many other types of leukemia.

Acquired mutation of the PIM1 gene

The protooncogene *PIM1*, which encodes the serine-threonine protein kinase, is located on chromosome 6p, and 2 cases had CNN-LOH in the region. All exons of the *PIM1* gene for these 2 cases were examined for mutations. As shown in Figure 1A, case #39 had a nucleic acid change of G to A at exon 4 of the *PIM1* gene leading to an amino acid change of glutamic acid (E) to lysine (K) at codon 135 (E135K). The amino acid change occurred between the ATP-binding site and serine-threonine kinase domain. The wild-type amino acid is conserved between human, rat, mouse and xenopus. Importantly, the complete remission sample of the same individual showed the wild-type sequence, demonstrating that the nucleic acid change was a disease-specific acquired alteration.

The missense mutation in the *PIM1* gene change produces the recognition site of a restriction enzyme, Hpy188III. A total of 34 t(8;21) AML samples and 40 normal blood DNA samples were examined for this mutation by Hpy188III digestion. The PCR product (178 bp) encompassing the mutation was only digested in case #39 (Figure 1B), but not the DNA from the other AML samples or normal blood DNA (*data not shown*), suggesting it is infrequent in the AML subtype. We also examined all exons of the *PIM1* gene by SSCP using 34 t(8;21) AML samples, but no shifted bands were detected other than exon 4 of case #39. The *PIM1* E135K mutant was also detected in B-cell diffuse large-cell lymphoma;[22] and another mutant (E135Q) was discovered in primary diffuse large B-cell lymphomas.[23] It remains to be clarified whether the E135K mutant is activated constitutively.

Prognostic significance of genomic change

Overall survival of t(8;21) AML patients of Group A (no genomic abnormality observed by SNP-chip) was significantly better than individuals in Group B (genomic abnormality observed by SNP-chip) (hazard ratio=2.992 [95% confidence interval, 1.247-7.179], p=0.01) (Figure 2). The event-free survival of individuals of Group A was also significantly better than those in Group B (hazard ratio=2.360 [95% confidence interval, 1.037-5.372], p=0.0347). We also compared the prognosis of individuals with the *KIT*-D816 mutation (6 cases) to those without the alteration (10 cases) in Group B, but found no significant difference (*data not shown*). These results strongly suggest that genomic changes in t(8;21) AML are associated with a poor overall and event-free survival.

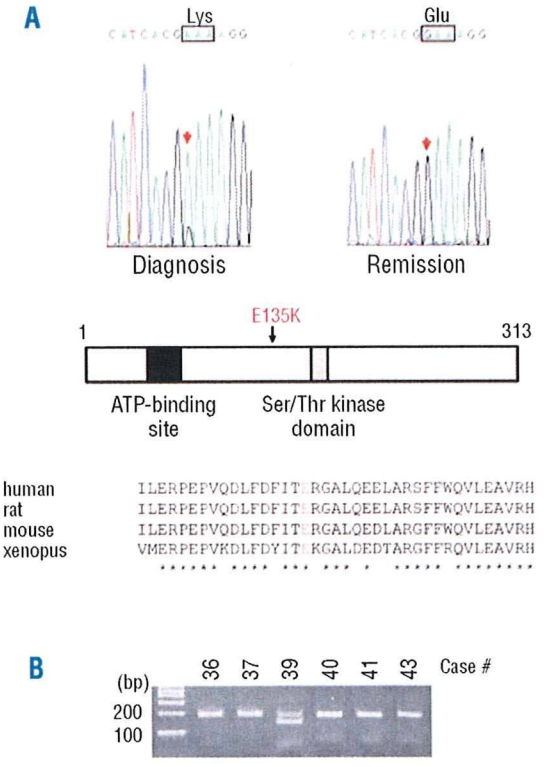

Figure 1. Acquired mutation of the *PIM1* gene in case #39. (A) Exon 4 of the *PIM1* gene in case #39 had a missense mutation in the sample at diagnosis but not at remission (top panel). The mutation leads to the amino acid change of glutamic acid (E) to lysine (K) at amino acid 135 (E135K) of PIM1 protein. This mutated amino acid is located between the ATP binding domain and serine-threonine kinase domain of the protein (middle panel). The wild-type amino acid (E) is highly conserved among human, rat, mouse and xenopus (bottom). Note, *identical amino acid. (B) The mutated DNA sequence produced a Hpy188III restriction enzyme recognition sequence. The region was amplified by PCR, digested with Hpy188III, and subjected to agarose gel electrophoresis. The PCR product from only case #39 was digested.

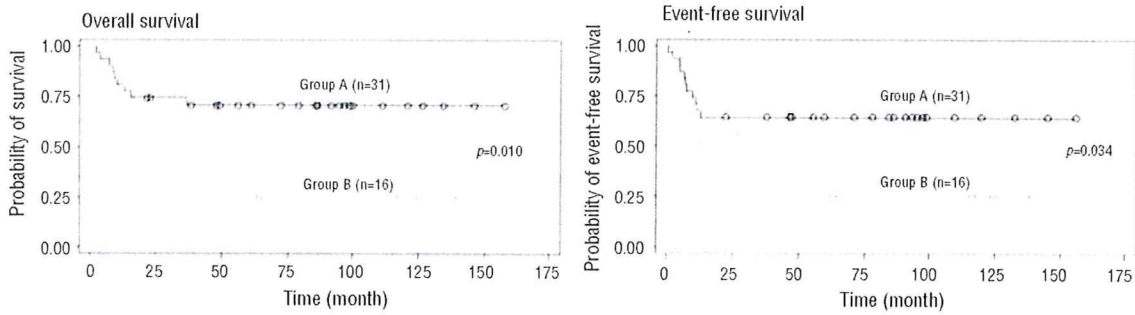

Figure 2. Comparison of overall survival and event-free survival of t(8;21) acute myeloid leukemia patients either with or without genomic changes. Overall survival (left) and event-free survival (right) were compared between Groups A and B. Black and grey lines indicate Group A (no genomic abnormality by SNP-chip) and Group B (genomic abnormality by SNP-chip), respectively.

A recent study showed that a *KIT*-D816V mutation is associated with a poor prognosis in t(8;21) AML patients.[9] Also, secondary cytogenetic abnormalities including trisomy of chromosome 8 and 4, deletion/duplication of chromosome 7, as well as deletion of chromosome X and Y in t(8;21) AML have previously been reported to be associated with a poor prognosis.[24] Taken together, these findings indicate that genomic alterations and *KIT*-D816 mutation confer a poor prognosis in t(8;21) AML patients. Further studies in a larger cohort of patients will begin to stratify prognostically the patients in relation to the genomic changes; and new therapeutic targets should be discovered.

Authorship and Disclosures

TA performed research, analyzed the data and wrote the paper; LS and DL determined mutation of genes; SO, MS, and YN performed SNP-chip analysis and developed CNAG; NK, SD, and JS assisted data analysis; JG and MM performed statistical analysis; VZ and AN performed the methylation analysis; SRM and RS performed FISH analysis; and SL and HPK directed the overall study. TA, LS and SO contributed equally in this work; and SL and HPK are co-last authors.

The authors reported no potential conflicts of interest.

References

1. Miyamoto T, Weissman IL, Akashi K. AML1/ETO-expressing nonleukemic stem cells in acute myelogenous leukemia with 8;21 chromosomal translocation. Proc Natl Acad Sci USA 2000;97:7521-6.
2. Mori H, Colman SM, Xiao Z, Ford AM, Healy LE, Donaldson C, et al. Chromosome translocations and covert leukemic clones are generated during normal fetal development. Proc Natl Acad Sci USA 2002;99:8242-7.
3. Wiemels JL, Xiao Z, Buffler PA, Maia AT, Ma X, Dicks BM, et al. In utero origin of t(8;21) AML1-ETO translocations in childhood acute myeloid leukemia. Blood 2002;99:3801-5.
4. Rhoades KL, Hetherington CJ, Harakawa N, Yergeau DA, Zhou L, Liu LQ, et al. Analysis of the role of AML1-ETO in leukemogenesis, using an inducible transgenic mouse model. Blood 2000;96:2108-15.
5. Fenske TS, Pengue G, Mathews V, Hanson PT, Hamm SE, Riaz N, et al. Stem cell expression of the AML1/ETO fusion protein induces a myeloproliferative disorder in mice. Proc Natl Acad Sci USA 2004;101:15184-9.
6. Yuan Y, Zhou L, Miyamoto T, Iwasaki H, Harakawa N, Hetherington CJ, et al. AML1-ETO expression is directly involved in the development of acute myeloid leukemia in the presence of additional mutations. Proc Natl Acad Sci USA 2001;98:10398-403.
7. Higuchi M, O'Brien D, Kumaravelu P, Lenny N, Yeoh EJ, Downing JR. Expression of a conditional AML1-ETO oncogene bypasses embryonic lethality and establishes a murine model of human t(8;21) acute myeloid leukemia. Cancer Cell 2002;1:63-74.
8. Care RS, Valk PJ, Goodeve AC, Abu-Duhier FM, Geertsma-Kleinekoort WM, Wilson GA, et al. Incidence and prognosis of c-KIT and FLT3 mutations in core binding factor (CBF) acute myeloid leukaemias. Br J Haematol 2003;121:775-7.
9. Schnittger S, Kohl TM, Haferlach T, Kern W, Hiddemann W, Spiekermann K, et al. KIT-D816 mutations in AML1-ETO-positive AML are associated with impaired event-free and overall survival. Blood 2006;107:1791-9.
10. Schessl C, Rawat VP, Cusan M, Deshpande A, Kohl TM, Rosten PM, et al. The AML1-ETO fusion gene and the FLT3 length mutation collaborate in inducing acute leukemia in mice. J Clin Invest 2005;115:2159-68.
11. Kuchenbauer F, Schnittger S, Look T, Gilliland G, Tenen D, Haferlach T, et al. Identification of additional cytogenetic and molecular genetic abnormalities in acute myeloid leukaemia with t(8;21)/AML1-ETO. Br J Haematol 2006;134:616-9.
12. Nannya Y, Sanada M, Nakazaki K, Hosoya N, Wang L, Hangaishi A, et al. A robust algorithm for copy number detection using high-density oligonucleotide single nucleotide polymorphism genotyping arrays. Cancer Res 2005;65:6071-9.
13. Yamamoto G, Nannya Y, Kato M, Sanada M, Levine RL, Kawamata N, et al. Highly sensitive method for genomewide detection of allelic composition in nonpaired, primary tumor specimens by use of affymetrix single-nucleotide-polymorphism genotyping microarrays. Am J Hum Genet 2007;81:114-26.

14. Kawamata N, Ogawa S, Zimmermann M, Kato M, Sanada M, Hemminki K, et al. Molecular allelokaryotyping of pediatric acute lymphoblastic leukemias by high-resolution single nucleotide polymorphism oligonucleotide genomic microarray. Blood 2008;111:776-84.
15. Raghavan M, Lillington DM, Skoulakis S, Debernardi S, Chaplin T, Foot NJ, et al. Genome-wide single nucleotide polymorphism analysis reveals frequent partial uniparental disomy due to somatic recombination in acute myeloid leukemias. Cancer Res 2005;65:375-8.
16. Gondek LP, Tiu R, O'Keefe CL, Sekeres MA, Theil KS, Maciejewski JP. Chromosomal lesions and uniparental disomy detected by SNP arrays in MDS, MDS/MPD, and MDS-derived AML. Blood 2008; 111: 1534-42.
17. Akagi T, Ogawa S, Dugas M, Kawamata N, Yamamoto G, Nannya Y, et al. Frequent genomic abnormalities in acute myeloid leukemia/myelodysplastic syndrome with normal karyotype. Haematologica 2009; 94:213-23.
18. Akagi T, Shih LY, Kato M, Kawamata N, Yamamoto G, Sanada M, et al. Hidden abnormalities and novel classification of t(15;17) acute promyelocytic leukemia (APL) based on genomic alterations. Blood 2009;113: 1741-8.
19. Downing JR, Head DR, Curcio-Brint AM, Hulshof MG, Motroni TA, Raimondi SC, et al. An AML1/ETO fusion transcript is consistently detected by RNA-based polymerase chain reaction in acute myelogenous leukemia containing the (8;21) (q22;q22) translocation. Blood 1993; 81:2860-5.
20. Shih LY, Liang DC, Huang CF, Chang YT, Lai CL, Lin TH, et al. Cooperating mutations of receptor tyrosine kinases and Ras genes in childhood core-binding factor acute myeloid leukemia and a comparative analysis on paired diagnosis and relapse samples. Leukemia 2008;22: 303-7.
21. Beghini A, Ripamonti CB, Castorina P, Pezzetti L, Doneda L, Cairoli R, et al. Trisomy 4 leading to duplication of a mutated KIT allele in acute myeloid leukemia with mast cell involvement. Cancer Genet Cytogenet 2000;119:26-31.
22. Pasqualucci L, Neumeister P, Goossens T, Nanjangud G, Chaganti RS, Küppers R, et al. Hypermutation of multiple proto-oncogenes in B-cell diffuse large-cell lymphomas. Nature 2001;412:341-6.
23. Montesinos-Rongen M, Van Roost D, Schaller C, Wiestler OD, Deckert M. Primary diffuse large B-cell lymphomas of the central nervous system are targeted by aberrant somatic hypermutation. Blood 2004;103: 1869-75.
24. Marcucci G, Mrózek K, Ruppert AS, Maharry K, Kolitz JE, Moore JO, et al. Prognostic factors and outcome of core binding factor acute myeloid leukemia patients with t(8;21) differ from those of patients with inv(16): a Cancer and Leukemia Group B study. J Clin Oncol 2005;23:5705-17.

Derivation of functional mature neutrophils from human embryonic stem cells

Yasuhisa Yokoyama,[1-3] Takahiro Suzuki,[1,2,4] Mamiko Sakata-Yanagimoto,[1-3] Keiki Kumano,[1,2] Katsumi Higashi,[5] Tsuyoshi Takato,[4] Mineo Kurokawa,[2] Seishi Ogawa,[1,4,6] and Shigeru Chiba[1,3]

[1]Department of Cell Therapy and Transplantation Medicine, University of Tokyo Hospital, Tokyo; [2]Department of Hematology and Oncology, Graduate School of Medicine, University of Tokyo, Tokyo; [3]Department of Clinical and Experimental Hematology, University of Tsukuba, Ibaraki; [4]Divison of Tissue Engineering, University of Tokyo Hospital, Tokyo; [5]Department of Clinical Hematology, School of Health Sciences, Kyorin University, Tokyo; and [6]The 21st Century COE Program, Graduate School of Medicine, University of Tokyo, Tokyo, Japan

Human embryonic stem cells (hESCs) proliferate infinitely and are pluripotent. Only a few reports, however, describe specific and efficient methods to induce hESCs to differentiate into mature blood cells. It is important to determine whether and how these cells, once generated, behave similarly with their in vivo–produced counterparts. We developed a method to induce hESCs to differentiate into mature neutrophils. Embryoid bodies were formed with bone morphogenic protein-4, stem cell factor (SCF), Flt-3 ligand (FL), interleukin-6 (IL-6)/IL-6 receptor fusion protein (FP6), and thrombopoietin (TPO). Cells derived from the embryoid bodies were cultured on a layer of irradiated OP9 cells with a combination of SCF, FL, FP6, IL-3, and TPO, which was later changed to granulocyte–colony-stimulating factor. Morphologically mature neutrophils were obtained in approximately 2 weeks with a purity and efficiency sufficient for functional analyses. The population of predominantly mature neutrophils (hESC-Neu's) showed superoxide production, phagocytosis, bactericidal activity, and chemotaxis similar to peripheral blood neutrophils from healthy subjects, although there were differences in the surface antigen expression patterns, such as decreased CD16 expression and aberrant CD64 and CD14 expression in hESC-Neu's. Thus, this is the first description of a detailed functional analysis of mature hESC-derived neutrophils. (Blood. 2009;113:6584-6592)

Introduction

Embryonic stem (ES) cells can self-renew and differentiate into cells derived from all 3 germ layers (ie, ectoderm, endoderm, and mesoderm). Both mouse and human ES cells give rise to mature blood cells of granulocyte/macrophage, erythroid, and megakaryoid lineages in vitro. For blood cell induction from ES cells, the majority of investigators use a coculturing system with mouse stromal cells such as S17[1] or OP9.[2,3] Embryoid body (EB) formation is also a commonly used method to obtain starting materials for further culture.[4-6] Cell surface antigens, such as CD45 and CD34, and colony-forming ability are used as blood cell markers. Hemangioblasts, which have the capacity to differentiate into both endothelial and blood cells, have also been produced.[7-9] Only a few studies, however, have achieved specific and effective induction of mature blood cells from ES cells, particularly human ES cells (hESCs).[10]

Human ESC-derived blood cells are potentially useful as a replacement for donation-based blood for transfusion in clinical settings, for drug discovery screening, and for monitoring drug efficacy and toxicity. The current blood donation system for transfusion is incapable of providing enough granulocytes for patients with life-threatening neutropenia, although granulocyte transfusion could have a potentially significant benefit for a certain population of severely neutropenic patients.[11,12] Given the large amount of neutrophils required for transfusion,[13] hESC-derived neutrophils might be a unique solution for this treatment demand. Therefore, the development of a highly effective method of neutrophil differentiation from hESCs is an important step for both clinical application of hESCs and granulocyte transfusion medicine.

The lack of an effective method for obtaining hESC-derived neutrophils with purity sufficient for functional analysis, however, has hampered progress in this field. Once neutrophils with a high purity can be generated from hESCs, it will be important to compare their activities with those of neutrophils produced in vivo, particularly given the fact that hESCs rarely give rise to hematopoietic stem cells in vitro,[14] and thus, that hESC-derived neutrophils might not be a progeny of hematopoietic stem cells. Here, we developed an effective method of deriving mature neutrophils from hESCs through EB formation and subsequent coculture with OP9, and analyzed their morphologic and phenotypic characteristics. We then performed functional analyses of hESC-derived neutrophils in vitro, focusing on superoxide production, phagocytosis, bactericidal activity, and chemotaxis, in comparison with peripheral blood neutrophils (PB-Neu's) obtained from healthy subjects.

Methods

Human ES cell culture and EB formation

In all experiments using hESCs, we used KhES-3[15] cells (a kind gift from Dr Nakatsuji; Kyoto University, Kyoto, Japan), which were maintained as previously described.[16] Briefly, KhES-3 colonies were cultured on irradiated mouse embryonic fibroblasts in Dulbecco modified Eagle medium/F12 (Invitrogen, Carlsbad, CA) supplemented with 20% KNOCKOUT serum

Submitted May 31, 2008; accepted March 5, 2009. Prepublished online as *Blood* First Edition paper, March 25, 2009; DOI 10.1182/blood-2008-06-160838.

An Inside *Blood* analysis of this article appears at the front of this issue.

The publication costs of this article were defrayed in part by page charge payment. Therefore, and solely to indicate this fact, this article is hereby marked "advertisement" in accordance with 18 USC section 1734.

replacer (Invitrogen) and 2.5 ng/mL human basic fibroblast growth factor (Invitrogen). The culture medium was replaced daily with fresh medium. Colonies were passaged onto new mouse embryonic fibroblasts every 6 days. To induce the formation of EBs, KhES-3 colonies were picked up using collagenase, and cultured in suspension in nonserum stem cell medium that we previously used in a hematopoietic stem cell expansion protocol.[17] After 24 hours, the colonies formed EBs, which were collected and cultured further for 17 days in Iscove modified Dulbecco medium (IMDM; Invitrogen) containing 15% fetal bovine serum (FBS), 1% nonessential amino acid (Invitrogen), 2 mM L-glutamine, 100 U/mL penicillin, 100 μg/mL streptomycin, and 0.1 mM 2-mercaptoethanol (ME) supplemented with cytokines (25 ng/mL bone morphogenic protein-4 [R&D Systems, Minneapolis, MN], 50 ng/mL stem cell factor [SCF; R&D Systems], 50 ng/mL Flt-3 ligand [R&D Systems], 50 ng/mL interleukin-6 [IL-6]/IL-6 receptor fusion protein [FP6; Kyowa Hakko Kirin, Tokyo, Japan], and 20 ng/mL thrombopoietin [TPO; Kyowa Hakko Kirin]).

Expansion of hematopoietic progenitor cells and terminal differentiation into mature neutrophils on OP9 stromal cells

OP9 cells (a kind gift from Dr Nakano; Osaka University, Osaka, Japan) were irradiated with 20 Gy and plated onto gelatin-coated 6-well tissue culture plates at a density of 1.5×10^5/well. The next day, the EBs (incubated for 18 days after the initiation of suspension culture) were trypsinized and disrupted into single cells. Cells were suspended in the progenitor expansion medium (IMDM supplemented with 10% FBS, 10% horse serum [StemCell Technologies, Vancouver, BC], 5% protein-free hybridoma medium [Invitrogen], 0.1 mM 2-ME, 100 U/mL penicillin, 100 μg/mL streptomycin, 100 ng/mL SCF, Flt-3 ligand, FP6, and 10 ng/mL TPO and IL-3 [R&D Systems]) and plated onto the irradiated OP9 cells (day 0). Each well contained up to 5×10^5 EB-derived cells. The culture medium was replaced with fresh medium on day 4.

On day 7 of the progenitor expansion phase, floating cells were collected, suspended with terminal differentiation medium (IMDM supplemented with 10% FBS, 0.1 mM 2-ME, 100 U/mL penicillin, 100 μg/mL streptomycin, and 50 ng/mL granulocyte colony-stimulating factor [G-CSF; Kyowa Hakko Kirin]), and transferred onto the newly irradiated OP9 cells. The culture medium was replaced with fresh medium on day 10. This terminal differentiation phase culture was continued for 6 or 7 days.

Preparation of normal PB-Neu's and bone marrow mononuclear cells

Human peripheral blood and bone marrow cells were obtained from healthy adult donors after obtaining informed consent in accordance with the Declaration of Helsinki. The institutional review board of the University of Tsukuba approved the use of peripheral blood neutrophils in this research. PB-Neu's were prepared as previously described.[18] The purity of the neutrophils was greater than 90%, with the remaining cells mainly eosinophils. Neutrophils were suspended in Hanks balanced salt solution (HBSS; Invitrogen) containing 0.5% bovine serum albumin (BSA) and placed at 4°C. In some experiments, peripheral blood mononuclear cells (PB-MNCs) were collected from the intermediate layer after centrifugation with Lymphoprep (Axis-shield, Oslo, Norway). Bone marrow cells were directly centrifuged with Lymphoprep, and only mononuclear cells were collected. Bone marrow mononuclear cells (BM-MNC's) were used immediately for RNA extraction.

Wright-Giemsa, myeloperoxidase, and alkaline-phosphatase staining

The morphology and granule characteristics of hESC-derived cells at the indicated days were assessed by Wright-Giemsa staining, comparing them with normal PB-Neu's. Myeloperoxidase and alkaline-phosphatase staining was performed using the New PO-K staining kit and alkaline phosphatase staining kit (MUTO PURE CHEMICALS, Tokyo, Japan). The prepared slides were inspected using an Olympus BX51 microscope equipped with a 100 × /1.30 UPlan objective lens (Olympus, Tokyo, Japan). Images were acquired with an HC-2500 digital camera and Photograb-2500 software (Fujifilm, Tokyo, Japan).

Electron microscopy

After 13 or 14 days culture, the population contained predominantly morphologically mature neutrophils, and was defined as hESC-Neu's. The hESC-Neu's and PB-Neu's were fixed in 2% paraformaldehyde/2.5% glutaraldehyde in 0.1 M phosphate buffered saline (PBS; Invitrogen) for at least 12 hours, and then postfixed in 1% osmium tetroxide in 0.1 M PBS for 2 hours. After fixation, samples were dehydrated in a graded ethanol series, cleared with propylene oxide, and embedded in Epon. Thin sections of cured samples were stained with uranyl acetate and Reynolds lead citrate. The sections were inspected using a transmission electron microscope, H7000 (Hitachi, Tokyo, Japan).

Semiquantitative RT-PCR for lactoferrin

Total RNA was obtained from hESC-derived cells of indicated culture days, PB-Neu's, PB-MNC's, and BM-MNC's using an RNeasy mini kit (QIAGEN, Hilden, Germany), and cDNA was synthesized from each RNA sample using a random primer and SuperScript III (Invitrogen) following the manufacturer's protocol. Semiquantitative polymerase chain reaction (PCR) was performed as previously described.[19] The sequence information of gene-specific primers used in reverse transcription (RT)–PCR and the PCR conditions is available upon request.

Flow cytometric analysis

Surface antigens of hESC-derived cells harvested on the indicated days were analyzed by flow cytometry using fluorescence-activated cell sorting (FACS) Aria (Becton Dickinson Immunocytometry Systems, San Jose, CA). Fc receptors on the cells were blocked with PBS containing 2% FBS and FcR Blocking Reagent (Miltenyi Biotec, Bergisch Gladbach, Germany). Antigens were stained with either fluorescein isothiocyanate (FITC)–conjugated antihuman CD13, CD64, CD11b (Beckman Coulter, Fullerton, CA), or CD14 (BD Pharmingen, San Diego, CA) antibodies; phycoerythrin-conjugated antihuman CD16, CD32, CD33 (Beckman Coulter), CD11b, or CD45 (BD Pharmingen) antibodies; or allophycocyanin-conjugated antihuman CD15, CD117 (BD Pharmingen), CD34, or CD133 (Myltenyi Biotec) antibodies. The negative range was determined by referencing the fluorescence of isotype controls. Dead cells were detected using 7-amino-actinomycin D (Via-Probe; BD Pharmingen).

Apoptosis assay

Neutrophils (hESC-Neu's and PB-Neu's) were suspended in IMDM with 0.5% BSA and incubated in 6-well plates at 37°C with 5% CO_2, with or without 50 ng/mL G-CSF. At the indicated time, neutrophils were harvested, stained with FITC-conjugated Annexin V and propidium iodide (PI) using an Annexin V-FITC Kit (Beckman Coulter), and analyzed by FACS Aria. Cells negative for both Annexin V and PI were judged as live cells.

G-CSF stimulation prior to assessing neutrophil function

Because the functions of hESC-Neu's are modified by G-CSF in the culture medium, we stimulated hESC-Neu's and PB-Neu's (PB-Neu(G+)'s) for 15 minutes at 37°C with 50 ng/mL G-CSF in the reaction medium. As a control, PB-Neu's without G-CSF stimulation (PB-Neu(G−)'s) were prepared. hESC-Neu's, PB-Neu(G+)'s, and PB-Neu(G−)'s were used for functional assays directly without changing the medium.

Detection of reactive oxygen species produced by neutrophils

Neutrophil production of reactive oxygen species was detected by flow cytometry using dihydrorhodamine123 (DHR; Sigma-Aldrich, St Louis, MO) as described previously.[20-22] Briefly, 1×10^5 hESC-Neu's, PB-Neu(G+)'s, or PB-Neu(G−)'s were suspended in 400 μL of the reaction medium (HBSS containing 0.5% BSA) per tube, and 3 tubes were prepared of each sample. Catalase (Sigma-Aldrich) at a final concentration of 1000 U/mL, 1.8 μL 29 mM DHR, and 100 μL 3.2 μM phorbol myristate

acetate (PMA; Sigma-Aldrich) were added to 1 of the 3 tubes; either no DHR or only DHR was added in the other 2 tubes as controls. Reaction medium was added to bring the final volume up to 500 μL. After 15-minute reaction at 37°C, the samples were washed twice with ice-cold reaction medium, and suspended in 200 μL reaction medium. Rhodamine fluorescence from the oxidized DHR was detected using FACS Aria.

Phagocytosis and NBT-reduction test using NBT-coated yeast cells

Phagocytosis and NBT reduction were visualized in a single set of experiments. Autoclaved Baker yeast was suspended in 0.5% NBT solution (0.5% NBT [Sigma-Aldrich] and 0.85% sodium chloride in distilled water) at a density of 1×10^8/mL. A 5-μL aliquot of this yeast suspension was added to hESC-Neu's, PB-Neu(G+)'s, and PB-Neu(G−)'s at 2.5×10^5 in 50 μL FBS. After 1 hour at 37°C, the samples were washed and stained with 1% safranin-O (MUTO PURE CHEMCALS) for 5 minutes. The samples were then washed twice and suspended in 100 μL PBS. A small aliquot of each sample was placed onto a glass slide and topped with a cover glass, and the number of ingested yeast cells and their change in color from brown to purple or black were examined using a microscope. Ingested yeast cells that changed color in the cells were counted as NBT-reaction positive, whereas those that were ingested but did not change color were counted as NBT-reaction negative. The phagocytosis rate was calculated as the percentage of neutrophils that contained one or more NBT-positive yeast cells. The phagocytosis score was calculated as the total number of positive yeast cells in 100 neutrophils. Only morphologically determined neutrophils were scored, excluding contaminating cells such as macrophages, the percentage of which was less than 15% of the total cells.

Bacterial killing assay

The bacterial killing assay was performed using *Escherichia coli* ATCC25922 as previously described[23] with some modifications. Briefly, 1×10^8 colony-forming units (CFUs) of exponentially growing bacteria were suspended in 1 mL HEPES-buffered saline with 10% human AB serum (MP Biomedicals, Irvine, CA) and opsonized at 37°C for 30 minutes. Neutrophils (hESC-Neu's, PB-Neu(G−)'s, and PB-Neu(G+)'s) were suspended in HEPES-buffered saline with 40% human AB serum at a concentration of 5×10^6/mL. The opsonized *E coli* was added to the suspension of hESC-Neu's and PB-Neu's, at a neutrophil/bacteria ratio of 2:1, or control medium. After 1-hour incubation, 50 μL of samples with and without neutrophils were diluted in 2.5 mL alkalinized water (pH 11) for lysis of neutrophils. Samples were further diluted with PBS, and duplicate aliquots were added to molten tryptic soy broth with 1.5% agar kept at 42°C, rapidly mixed, and plated on dishes. The CFUs were counted after overnight incubation.

Chemotaxis assay

Chemotactic ability was determined using a modified Boyden chamber method.[24] Briefly, 700 μL of the reaction medium (HBSS containing 0.5% BSA) with or without 10^{-7} M formyl-Met-Leu-Phe (fMLP; Sigma-Aldrich) was placed into each well of a 24-well plate, and the cell culture insert (3.0-μm pores; Falcon; Becton Dickinson, Franklin Lakes, NJ) was gently placed into each well to divide the well into upper and lower sections. Neutrophils were suspended in the reaction medium at 2.5×10^6/mL and 200 μL cell suspension was added to the upper well, allowing the neutrophils to migrate from the upper to the lower side of the membrane for 90 minutes at 37°C. After incubation, the membranes were washed, fixed with methanol, stained with Carrazi hematoxylin (MUTO PURE CHEMICALS), and mounted on the slide glass. The number of neutrophils that migrated through the membrane from the upper to the lower side was counted using a microscope with a high-power lens (× 400) in 3 fields: 2 near the edge and 1 on the center. Only mature neutrophils were counted.

Statistical analyses

Results are expressed as mean plus or minus SD. Statistical significance was determined using a 2-tailed Student *t* test. Results were considered significant when *P* values were less than .05.

Results

Effective derivation of mature neutrophils from hESCs with high purity

After initiating the suspension culture of EB-derived cells, small clusters of round-shaped cells appeared on the OP9 stromal layer around day 4. The morphology of the day-7 cells visualized with Wright-Giemsa staining suggested that they were myeloblasts and promyelocytes. On days 9 and 11, myelocytes and metamyelocytes were predominant, and on day 13 or 14, 70% to 80% of the cells appeared to be stab and segmented neutrophils (Figure 1A), with approximately 90% of the granulocytes at the metamyelocyte stage or later (Table 1). This finding indicated that hESC-derived cells differentiated into mature neutrophils by a process similar to physiologic granulopoiesis. The remaining cells appeared to be macrophages or monocytes, and cells of other lineages, such as erythroid or lymphoid cells, were not observed at any time during the culture. The number of total cells peaked around days 9 to 11, with an average 2.9-fold increase (range; 0.5- to 10.0-fold in 23 independent cultures) compared with the initial EB-derived cell number. The final yield of the cells on day 13 or 14 was 1.7-fold (range; 0.1- to 8.8-fold in 28 independent cultures). We attempted to further purify the hESC-derived mature neutrophils from the "hESC-Neu" population using density gradient methods, but higher purification could not be achieved without massively reducing the cell yield. We therefore used hESC-Neu's in the subsequent experiments.

Most (97.3% ± 1.5%) of the hESC-derived mature neutrophils defined by Wright-Giemsa staining were positive for myeloperoxidase, and the alkaline-phosphatase score of hESC-Neu's was 284 plus or minus 8.6 (Figure 1B). Under transmission electron microscopy, segmented nuclei and round cytoplasmic granules of hESC-Neu's appeared very similar to those in PB-Neu's (Figure 1C).

Some myeloid cell lines, such as HL-60, have abnormal biosynthesis of secondary granule proteins.[25,26] Thus, it is important to verify the biosynthesis of secondary granule proteins in hESC-Neu's. The levels of lactoferrin mRNA in hESC-derived cells at different stages were compared with those in PB-Neu's and BM-MNCs by semiquantitative RT-PCR (Figure 1D). Lactoferrin biosynthesis begins at the myelocyte stage and terminates by the beginning of the band stage.[25,27] Lactoferrin mRNA was not detected in PB-Neu's from some donors, but was detected in PB-Neu's from others. Human ESC–derived cells at various stages as well as BM-MNCs expressed lactoferrin mRNA. The expression level of lactoferrin mRNA in the hESC-derived cells was highest at day 10 of the induction culture and declined on days 13 and 14. These findings are consistent with the documented pattern of lactoferrin biosynthesis.

Surface antigen presentation in comparison to PB-Neu's

Surface antigen expression at each level of differentiation of hESC-derived cells was analyzed by flow cytometry (Figure 2). From days 7 to 13, the common blood cell antigen CD45 was expressed in almost all the cells. CD34, CD117, and CD133, cell surface markers on normal immature hematopoietic cells, were detected in a small population of the cells on day 7, but disappeared by day 10. Common myeloid antigens CD33 and CD15 were also highly expressed, whereas CD11b expression increased during the course of maturation. CD13 is also a common myeloid antigen, but

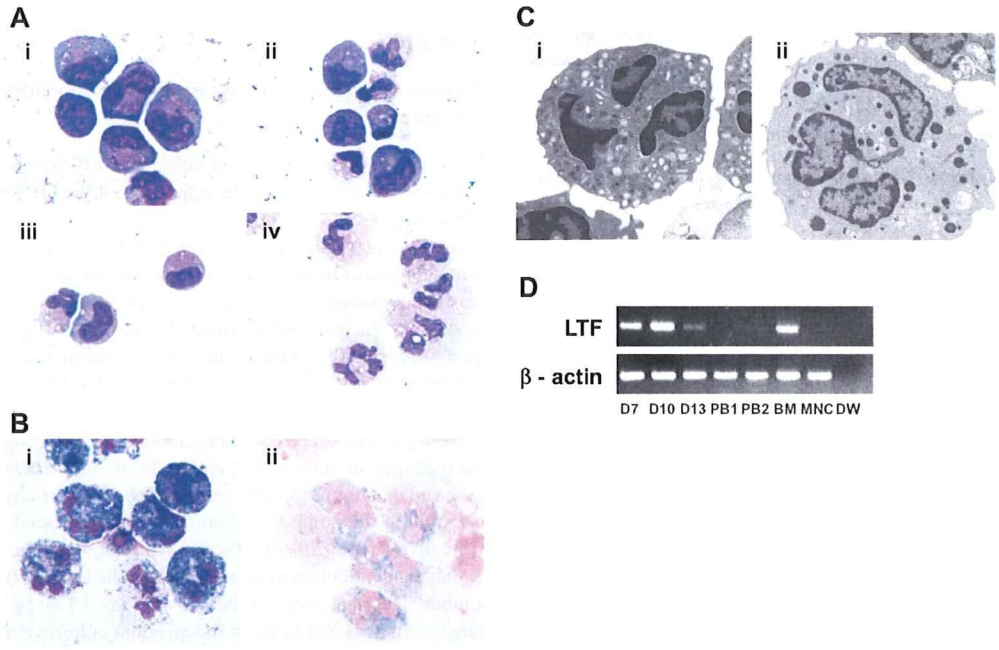

Figure 1. Morphology of hESC-derived cells and expression of lactoferrin mRNA. (A) Wright-Giemsa staining of the day-7 cells (i) revealed that they were morphologically myeloblasts and promyelocytes. On days 9 (ii) and 11 (iii), myelocytes and metamyelocytes were predominant, and on day 13 (iv; hESC-Neu), 70% to 80% of the cells appeared to be stab and segmented neutrophils. Original magnification, ×1000. (Bi) 97.3% plus or minus 1.5% of hESC-Neu's were myeloperoxidase positive. (ii) The neutrophil alkaline-phosphatase score in hESC-Neu's was 284 plus or minus 8.6. Values represent mean plus or minus SD. Original magnification, ×1000. (C) Microstructure of hESC-Neu's. Similar to steady-state neutrophils separated from peripheral blood (i), segmented nuclei and cytoplasmic granules were observed in hESC-Neu's (ii). Original magnification, ×8000. (D) Lactoferrin (LTF) mRNA was expressed in hESC-derived cells on day 7 (D7), peaked on day 10 (D10), and was weakly positive on day 13 (D13). Bone marrow mononuclear cells (BM) were strongly positive for LTF mRNA, but PB-Neu's (PB1 and 2) were negative, although faint bands were detected in PB-Neu's prepared from some donors (data not shown). As a negative control, peripheral blood mononuclear cells (MNCs) were used.

its expression was observed in less than 20% of the cells on day 7 and did not subsequently increase. CD16 (Fcγ receptor (FcγR) III), which is expressed in neutrophils as well as natural killer cells, macrophages, and a small subset of monocytes,[28] was already expressed by day 7, and increased with maturation. This expression pattern of CD16 is consistent with that during normal neutrophil differentiation, although the proportion of $CD16^+$ cells was lower than that of morphology-defined mature neutrophils on day 13. The ratio of CD32 (FcγRII)–positive cells increased as the differentiation stage advanced, and eventually reached 90%. CD64 (FcγRI) expression was greater than 80%, peaking on day 10, and the high percentage was maintained through day 13. CD14 was expressed in 20% to 25% of the cells on days 10 and 13.

Table 1. Differentiation pattern of hESC-derived cells

	% of total cells		
Cell type	Day 7	Day 10	Day 13
Myeloblasts	61.0 ± 9.1	2.3 ± 1.2	ND
Promyelocytes	16.8 ± 6.3	8.5 ± 0.9	0.7 ± 0.8
Myelocytes	12.3 ± 4.8	34.0 ± 6.8	6.4 ± 3.4
Metamyelocytes	3.0 ± 1.0	19.0 ± 1.3	10.2 ± 4.3
Stab neutrophils	0.8 ± 0.3	16.2 ± 3.0	18.3 ± 2.6
Segmented neutrophils	0.3 ± 0.6	14.7 ± 6.0	53.1 ± 9.6
Macrophage/monocytes	5.7 ± 0.6	5.3 ± 1.3	11.2 ± 1.4
Mature neutrophils	1.2 ± 0.8	30.8 ± 4.6	71.4 ± 7.4

The sum of the stab and segmented neutrophils indicates the total mature neutrophils. Data are shown as mean plus or minus SD (n = 3 independent experiments).

ND indicates not detectable.

In normal peripheral blood, both neutrophils and monocytes express CD15 and CD11b. In addition, mature neutrophils express CD16, whereas monocytes express CD14.[28,29] Detailed analysis on day 13 revealed that approximately 70% of $CD15^+$ and $CD11b^+$ cells were $CD16^+$, and almost all $CD15^+$ and $CD16^+$ cells expressed CD11b (Figure 2Bi,ii). Given that 70% to 80% of the cells on day 13 were morphologically mature neutrophils (Table 1), it is likely that the majority of hESC-Neu's had CD15, CD11b, and CD16 expression patterns similar to PB-Neu's, although some hESC-Neu's did not express CD15 or CD16, particularly CD16.

CD32 is broadly expressed on myeloid cells, whereas CD64 is expressed only on monocytes but not on neutrophils in the peripheral blood.[28] In the bone marrow, CD64 expression is observed in a small population of myeloblasts, peaks at the promyelocyte, myelocyte, and metamyelocyte stages, and then diminishes, although a small proportion of the stab neutrophils still express CD64.[30,31] We confirmed that virtually no PB-Neu's expressed CD64 (data not shown). In contrast, almost all $CD15^+$ and $CD16^+$ hESC-Neu's expressed CD64 on day 13, indicating that both stab and segmented hESC-Neu's expressed CD64, because segmented neutrophils represented more than 50% of the cells on day 13 (Figure 2Biii; Table 1). Nearly 50% of $CD15^+$ and $CD16^+$ cells were weakly positive for CD14, in contrast to the negative expression of CD14 in steady-state PB-Neu's (Figure 2Biv). This aberrant expression of CD64 and CD14 in hESC-Neu's is similar to their positive expression on some of the neutrophils harvested from healthy donors who received G-CSF administration[32,33] and the neutrophils derived from bone marrow $CD34^+$ cells in vitro by G-CSF stimulation.[31]

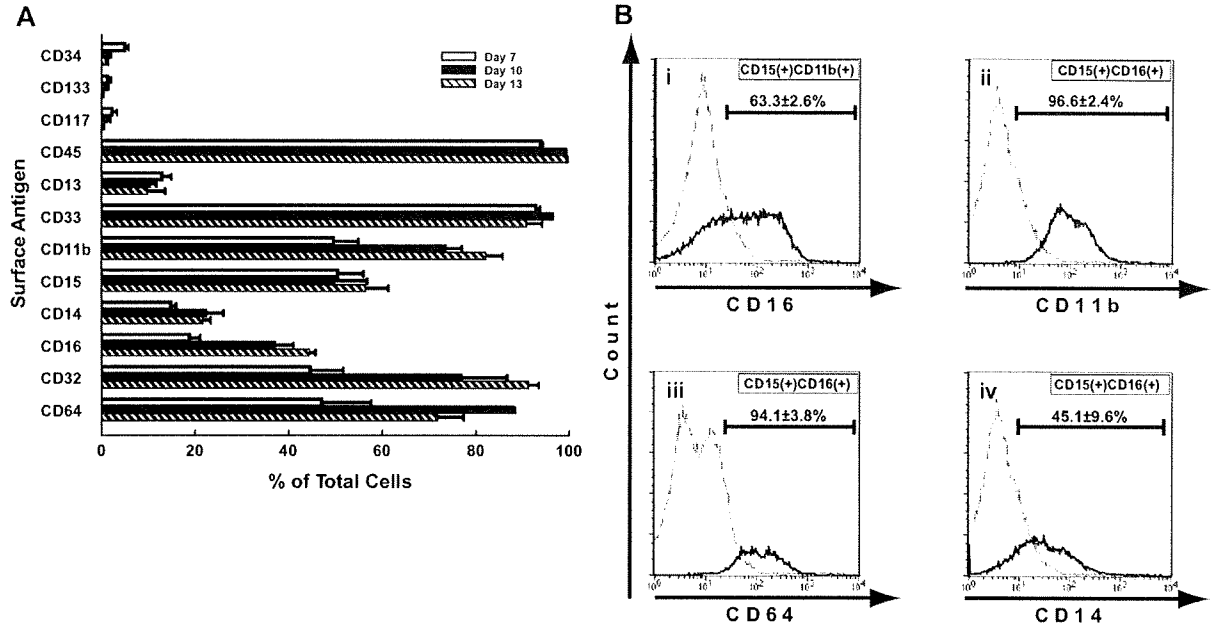

Figure 2. Surface antigens of hESC-derived cells. (A) Surface antigen expression at each level of differentiation of hESC-derived cells was analyzed by flow cytometry. CD45 was expressed in almost all the cells. CD34, CD117, and CD133, immature markers of hematopoiesis, were detected in a small population of the cells on day 7, and had almost disappeared by day 10. Common myeloid antigens CD33 and CD15 were highly expressed, and the expression of CD11b increased during maturation. CD13 was expressed in less than 20% of the cells throughout the culture period. The expression of CD16, a mature neutrophil marker, increased following maturation, but was observed in only approximately 45% of the cells, even on day 13. CD14 and CD64 expression was aberrantly observed in some cells. Bars represent SDs (n = 3). (B) In the steady state, mature neutrophils in peripheral blood were $CD15^+$, $CD11b^+$, and $CD16^+$. (i) In hESC-derived cells on day 13, 63.3% plus or minus 2.6% of the $CD15^+$ and $CD11b^+$ cells were $CD16^+$, and (ii) almost all of the $CD15^+$ and $CD16^+$ cells were $CD11b^+$. (iii-iv) On the other hand, CD64 and CD14 were rarely expressed on mature neutrophils in the peripheral blood. $CD15^+$ and $CD16^+$ cells from hESCs, consistent with the phenotype of mature neutrophils, showed aberrant expression of CD64 (iii) and CD14 (iv), in 94.1% plus or minus 3.8% and 45.1% plus or minus 9.6% of the cells, respectively. Data are presented as mean plus or minus SD (n = 3).

Apoptosis pattern and prolonged survival by G-CSF of hESC-Neu's and PB-Neu's

In the steady state, PB-Neu's have a short life span of approximately 24 hours, but this can be prolonged by G-CSF stimulation.[34] Some hESC-Neu's were already apoptotic at the time of harvest and therefore we focused on the nonapoptotic fraction of hESC-Neu's (Figure 3). In contrast to the PB-Neu's, which underwent apoptosis within 6 hours without G-CSF, consistent with previous reports,[34] a proportion of apoptotic cells among hESC-Neu's in the medium without G-CSF did not increase for up to 6 hours after the start of the culture. In addition, there were no differences between the cultures with and without G-CSF for up to 6 hours. After 6 hours, however, there was a more rapid decrease in nonapoptotic cells in hESC-Neu's without G-CSF than in hESC-Neu's with G-CSF, which resulted in a lower number of viable cells than hESC-Neu's with G-CSF at 24 hours, although the number of viable cells of hESC-Neu's without G-CSF was still higher than that of PB-Neu's without G-CSF.

Oxidative burst phenotype was similar in hESC-Neu's and PB-Neu's

Oxidative burst is an essential function of neutrophils when killing microorganisms, but an inappropriate burst sometime causes injury to the host tissue. We assessed the ability to convert DHR to rhodamine in hESC-Neu's and PB-Neu's using flow cytometry.[20] Because G-CSF, which could substantially affect the result, was used during the culture, we compared hESC-Neu's with PB-Neu(G+)'s and PB-Neu(G−)'s as described in "G-CSF stimulation prior to assessing neutrophil function." When DHR was added to the neutrophil suspensions, rhodamine-specific fluorescence was detected in hESC-Neu's, and in PB-Neu(G−)'s and PB-Neu(G+)'s without PMA stimulation, indicating basal superoxide production without PMA stimulation in each neutrophil preparation (Figure 4). PMA stimulation increased rhodamine mean fluorescence intensity in hESC-Neu's, but to a lesser extent than in PB-Neu(G−)'s and PB-Neu(G+)'s. Consequently, the mean rhodamine fluorescence intensity after PMA stimulation was similar in hESC-Neu's, PB-Neu(G−)'s, and PB-Neu(G+)'s, suggesting that the maximum superoxide production is comparable between hESC-Neu's and PB-Neu's.

Phagocytosis and subsequent NBT reduction activity, and bactericidal activity were similar between hESC-Neu's and PB-Neu's

Neutrophils protect against infectious microorganisms by phagocytosing and subsequently killing them. These functions of hESC-Neu's and PB-Neu's were evaluated in an experimental system using NBT-coated yeast. Under the microscope, mature neutrophils could be easily distinguished from contaminating macrophages by the unique shape of their nuclei after 1% safranin-O staining (Figure 5A). NBT-coated yeast that had not been ingested had a red-brown color that began to change to purple or black, beginning at the periphery, and eventually became completely black, because the NBT coating on the yeast was reduced by neutrophils after phagocytosis. Thus, neutrophils that had phagocytosis and NBT-reducing ability could be easily identified. hESC-Neu's had a slightly lower phagocytosis rate than PB-Neu(G−)'s and PB-Neu(G+)'s (Figure 5B). The phagocytosis score, however, was not significantly different between hESC-Neu's and PB-Neu(G−)'s and PB-Neu(G+)'s (Figure 5C). The cells on day 8 of the culture, most of which were morphologically myeloblasts and promyelocytes, were rarely observed

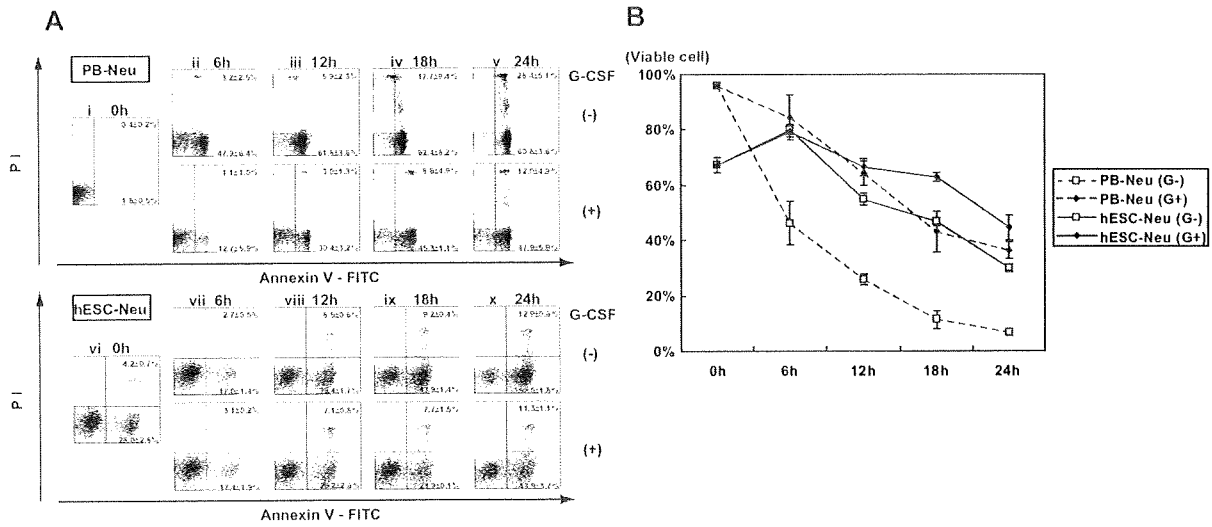

Figure 3. Apoptosis pattern and G-CSF effect on survival of hESC-Neu's. (A) Flow cytometric analysis. In the steady state, PB-Neu's have a short life span of approximately 24 hours, but this can be prolonged by G-CSF stimulation (i-v). Some hESC-Neu's were already apoptotic at the time of the harvest from the induction culture (vi). In contrast to the PB-Neu's that underwent apoptosis within 6 hours without G-CSF (ii), the proportion of apoptotic cells did not increase for up to 6 hours after the start of the culture of hESC-Neu's in the medium without G-CSF (vi,vii). In addition, there were no differences between the cultures of hESC-Neu's with and without G-CSF for up to 6 hours (vii). After 6 hours, nonapoptotic cells decreased more rapidly among hESC-Neu's without G-CSF than among hESC-Neu's with G-CSF (viii-x), resulting in the lower number of viable cells than hESC-Neu's with G-CSF at 24 hours (x). Figures are representative of 3 independent experiments. Data are presented as mean plus or minus SD (n = 3). (B) The time course of the decrease in viable cells. Bars represent SDs (n = 3).

to phagocytose the yeast or reduce NBT if they had ingested the yeast, indicating that we observed phagocytosis and NBT reduction that was specific to mature neutrophils.

Because the hESC-Neu's had sufficient phagocytosing ability and superoxide production, we next investigated whether hESC-Neu's can kill bacteria. The bactericidal activity of hESC-Neu's and PB-Neu's was compared using *E coli*. When incubated with hESC-Neu's and PB-Neu(G−)'s and PB-Neu(G+)'s, the numbers of CFUs were similarly reduced to approximately 40% that of the control, indicating comparable bactericidal activity against *E coli* between hESC-Neu's and PB-Neu's (Figure 5D).

Chemotaxis was similar between hESC-Neu's and PB-Neu's

We compared chemotaxis of hESC-Neu's and PB-Neu's using a modified Boyden chamber method. After incubation with or without fMLP in the lower well, neutrophils had migrated from the upper side to the lower side of the membrane. Neutrophil migration without fMLP in the lower well was considered random migration. The number of neutrophils that migrated randomly was not significantly different between hESC-Neu's and PB-Neu(G−)'s, but PB-Neu(G+)'s showed significantly more random migration than the others (Figure 5E). The number of migrated cells increased in hESC-Neu's, PB-Neu(G−)'s, and PB-Neu(G+)'s when fMLP was added in the lower well. The increase in cell migration induced by chemotaxis to fMLP was calculated by subtracting the number of randomly migrated cells without fMLP from that of migrated cells with fMLP. There were no significant differences between hESC-Neu's and PB-Neu(G−)'s or PB-Neu(G+)'s in the net fMLP-induced chemotaxis.

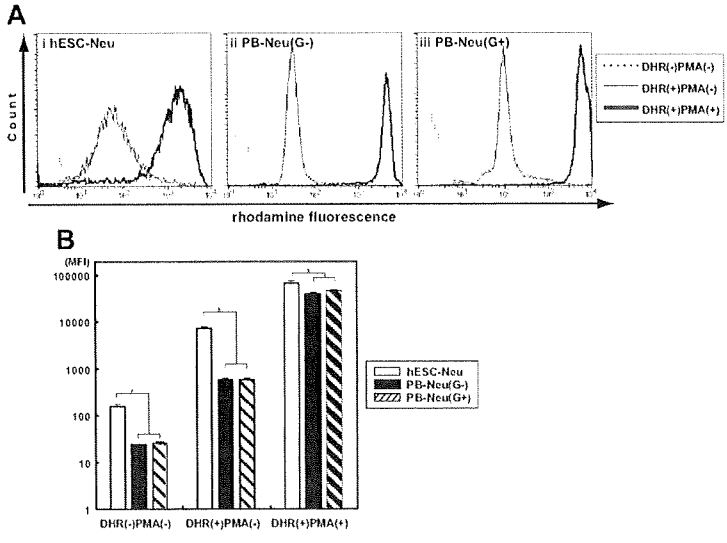

Figure 4. Superoxide production of hESC-Neu's assessed by dihydrorhodamine123 oxidation. (A) Dihydrorhodamine123 (DHR) was reacted to neutrophils with or without phorbol myristate acetate (PMA), and the resultant rhodamine fluorescence was detected by flow cytometry. When DHR was added to the reaction medium without PMA (line), the fluorescence levels were slightly elevated in hESC-Neu's (i), PB-Neu(G−)'s (ii), and PB-Neu(G+)'s (iii). The addition of PMA dramatically increased the levels of fluorescence in all 3 neutrophil preparations (bold line). The figures are representative of 3 independent experiments. (B) Comparison of superoxide production between hESC-Neu's and PB-Neu's using mean fluorescence intensity (MFI) of rhodamine. When DHR was added without PMA stimulation, rhodamine-specific fluorescence was detected in hESC-Neu's, PB-Neu(G−)'s, and PB-Neu(G+)'s. PMA stimulation increased rhodamine MFI in hESC-Neu's though to a lesser extent than in PB-Neu(G−)'s and PB-Neu(G+)'s. Consequently, rhodamine MFI after PMA stimulation was similar in hESC-Neu's, PB-Neu(G−)'s, and PB-Neu(G+)'s, suggesting that the maximum superoxide production was comparable between hESC-Neu's and PB-Neu's (n = 3; bars represent SDs; $^*P < .05$ compared with hESC-Neu's).

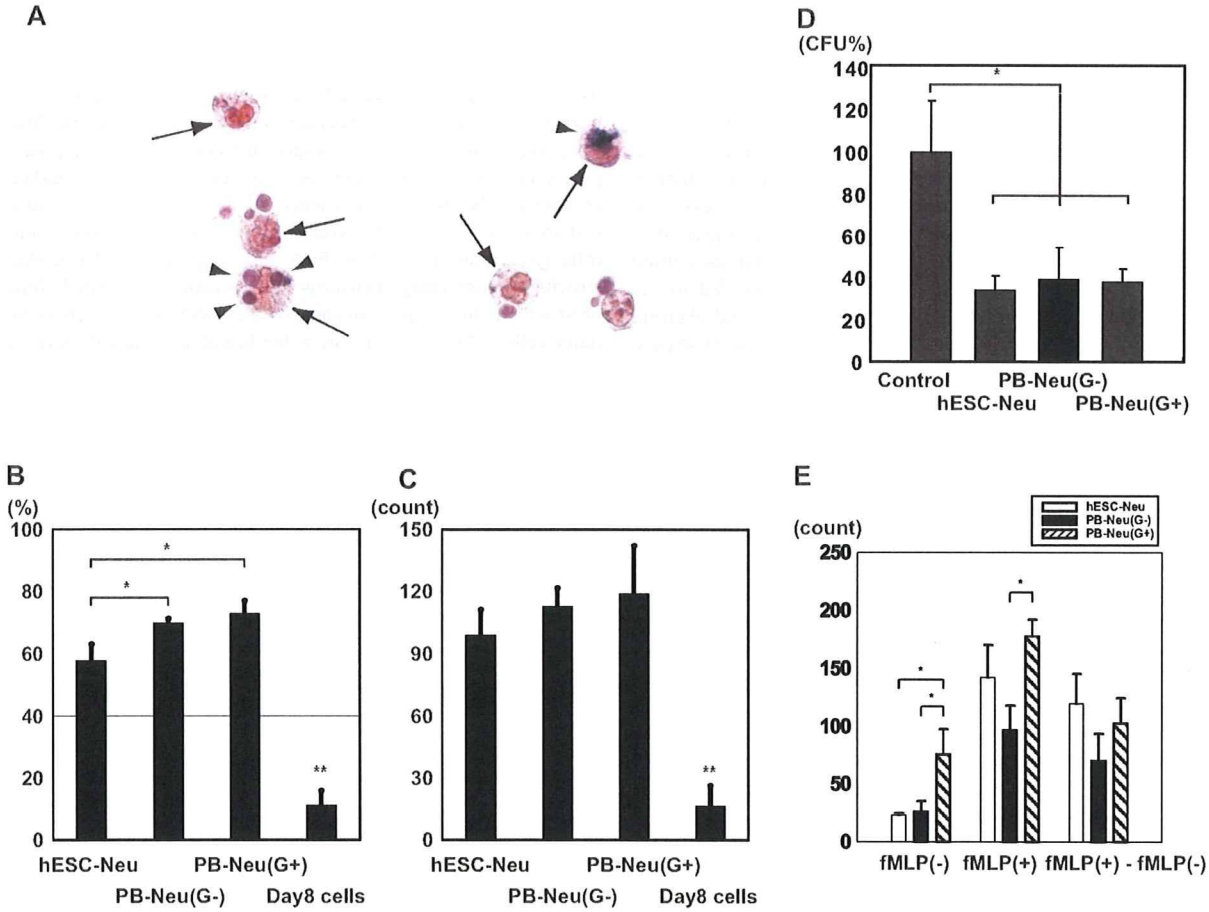

Figure 5. NBT-coated yeast cell-phagocytosis test, bactericidal activity, and chemotaxis assay. (A) NBT-coated yeast cells were added to a neutrophil suspension and incubated at 37°C. After 1 hour, the cells were stained with 1% safranin-O, and observed using a microscope. Mature neutrophils (➔) could be easily distinguished from contaminating macrophages (white arrow; only the nucleus is observed in the figure) by the unique shape of their nuclei. Yeast cells were red-brown in color before being ingested (white arrowhead); the color began to change to purple or black beginning at the periphery of the yeast cell, and eventually became completely black (➤) because the NBT was reduced after ingestion. Yeast cells that changed color in the cells were counted as NBT-reduction positive. Original magnification, ×400. (B) The phagocytosis rate was calculated as a percentage of the neutrophils that contained one or more yeast cells. hESC-Neu's had a slightly lower phagocytosis rate than that of PB-Neu(G−)'s and PB-Neu(G+)'s. (C) The phagocytosis score was calculated as the total number of positive yeast cells in 100 neutrophils. There were no significant differences in the phagocytosis score between hESC-Neu's and PB-Neu(G−)'s or PB-Neu(G+)'s. The cells on day 8 of the culture (day-8 cells) were rarely observed to phagocytose the yeast cells or reduce NBT. (In B-C, n = 3; bars indicate SDs; $^*P < .05$ compared with PB-Neu(G−)'s and PB-Neu(G+)'s; $^{**}P < .05$ compared with hESC-Neu's, PB-Neu(G−)'s, and PB-Neu(G+)'s.) (D) Bactericidal assay. *E coli* was opsonized with human AB serum, and incubated with hESC-Neu's, PB-Neu(G−)'s, PB-Neu(G+)'s, or control medium. After 1-hour incubation with hESC-Neu's, PB-Neu(G−)'s, and PB-Neu(G+)'s, the colony-forming units (CFUs) were significantly reduced to approximately 40% of the control. There were no significant differences in bactericidal activity between hESC-Neu's, PB-Neu(G−)'s, and PB-Neu(G+)'s. The CFUs of controls are presented as 100% (n = 3; bars indicate SDs; $^*P < .05$ compared with control). (E) Chemotaxis assay by a modified Boyden chamber method. The number of neutrophils that migrated randomly (fMLP(−)) was not significantly different between hESC-Neu's and PB-Neu(G−)'s, but PB-Neu(G+)'s showed significantly greater random migration than hESC-Neu's and PB-Neu(G−)'s. The number of migrating cells increased in all hESC-Neu's, PB-Neu(G−)'s, and PB-Neu(G+)'s when fMLP was added to the lower well (fMLP(+)). The increase in the number of migrating cells induced by chemotaxis to fMLP (fMLP(+)-fMLP(−)) was not significantly different between hESC-Neu's and PB-Neu(G−)'s or PB-Neu(G+)'s (n = 3; bars indicate SDs; $^*P < .05$).

Discussion

We developed a specific and effective method for deriving mature neutrophils from hESCs, making it possible to analyze hESC-derived neutrophils in detail. hESC-derived neutrophils had characteristics similar to steady-state peripheral blood mature neutrophils in morphology and essential functions, although there were some differences in surface antigen expression.

Unfortunately, attempts to further purify the hESC-derived mature neutrophils from the hESC-Neu population by density gradient methods led to a massive reduction in cell yield. In the flow cytometric analysis, the mean intensity of hESC-Neu's in forward scatter was higher than that of PB-Neu's (data not shown), indicating that the size of morphologically mature neutrophils, comprising 70% to 80% of the hESC-Neu population, was larger than that of PB-Neu's. This finding indicates that the density of morphologically mature neutrophils in the hESC-Neu population was lower than that of PB-Neu's, which made it difficult to separate hESC-Neu's from other contaminating cells.

In this culture, we observed morphologically defined myeloblasts, promyelocytes, myelocytes, metamyelocytes, and, eventually, mature stab and segmented neutrophils, in this order, during the 13-day culture, which is similar to the granulocyte maturation process in bone marrow. The surface antigen expression pattern during differentiation was similar to that during normal granulopoiesis, with CD34 and CD117 expression on immature cells, and an increase in CD16 expression as differentiation advanced. Most

hESC-Neu's expressed CD16, CD15, CD11b, CD33, and CD45. This pattern is consistent with normal PB-Neu's, but the percentage of CD16-expressing cells was lower than that of mature neutrophils determined by morphology. The lower CD16 expression level is documented in neutrophils derived in vitro from bone marrow $CD34^+$ cells by stimulation with G-CSF, and is considered to be the effect of G-CSF on myeloid progenitors.[31] G-CSF also induces CD64 and CD14 expression on mature neutrophils,[31,35] and these effects are also observed in vivo when G-CSF is administered to healthy volunteers.[32,33] Therefore, the G-CSF present in the culture from day 7 may have affected the progenitors and led to the relatively low expression of CD16 on hESC-Neu's and aberrant expression of CD64 and CD14 on $CD15^+$ and $CD16^+$ hESC-Neu's.

In the apoptosis assay, some hESC-Neu's were already apoptotic at the time of the harvest from the induction culture, but the proportion of apoptotic cells among hESC-Neu's in the medium without G-CSF did not increase for up to 6 hours after the start of the culture. There are 2 possible reasons for the difference in the rate of apoptosis. First, the hESC-Neu's were more heterogeneous than the PB-Neu's, as they comprised cells at different stages from incompletely differentiated cells such as metamyelocytes to maturation-completed and aged neutrophils. Relatively immature cells or unaged mature neutrophils in the hESC-Neu population might have a longer lifespan than PB-Neu's. Second, the effect of G-CSF used in the induction culture might continue even after the washout.

In the chemotaxis assay, the random migration of hESC-Neu's was almost the same as that of PB-Neu(G−)'s, but lower than that of PB-Neu(G+)'s, although hESC-Neu's were stimulated by G-CSF before the assay. The effect of G-CSF on the random migration of neutrophils is controversial; random migration increases in vitro when neutrophils are stimulated by G-CSF,[36] whereas neutrophils obtained from G-CSF–treated patients with nonmyeloid malignancies show decreased random migration and chemotaxis.[37,38] Our in vitro experiment with PB-Neu(G+)'s and PB-Neu(G−)'s replicated the former result. Nevertheless, hESC-Neu's showed relatively low random migration despite stimulation with G-CSF, while maintaining almost normal fMLP-induced chemotaxis. One possible reason for these differences might be the continuous stimulation by G-CSF; hESC-Neu's were stimulated from the myeloblast stage, and thus, it was expected that the characteristics of the hESC-Neu's were more similar to those of neutrophils from G-CSF–stimulated donors rather than to normal mature neutrophils.

The low yield of hESC-Neu's is a major obstacle to their functional analysis in animals, and further, to their potential use in drug screening and clinical applications. The number of hESC-Neu's produced was less than twice that of the input EB-derived cells. Recently, erythroid progenitor cell lines that could differentiate into functional mature red blood cells both in vitro and in vivo were established from mouse ESCs.[39] In that report, the starting number of ESCs required to establish one progenitor line was 5×10^5, and transplantation of 2×10^7 cells of the progenitor line could ameliorate anemia in mice by increasing the red blood cell count. Similar methods could be considered in the granulopoiesis from hESCs. Another potential method is to use more immature or proliferation-competent cells than the cells with which we initiated the induction culture. One candidate may be hematopoietic progenitors that emerge in saclike structures derived from ESCs. In a report using cynomolgus monkey ESCs,[40] EBs were created and subsequently subjected to adherent culture on a gelatin-coated dish. After 2 weeks, saclike structures emerged that contained hematopoietic precursors at various stages of myeloid lineage. The authors mentioned the possible existence of hemangioblasts, because endothelial cells could be produced from those precursors under different conditions. Others have also reported similar saclike structures containing hematopoietic precursors created from hESCs.[10] In this paper, megakaryocytes were created from the inner cells, which were positive for hematoendothelial markers, such as CD34, CD31, vascular endothelial growth factor-receptor 2, and vascular endothelial-cadherin. These similar findings suggest that the cells in the saclike structures contain cells that are more immature than our EB-derived cells, and that the precursors inside the saclike structures have greater proliferation potency than our EB-derived cells. Because neither paper directly demonstrated the efficiency of mature blood cell production from monkey or human ES cells, however, the efficiency of producing neutrophils from our EB-derived cells should be compared with that from the saclike structure–derived cells.

Acknowledgments

We thank Dr Nakatsuji for providing the KhES-3, and Dr Nakano for providing the OP9 cells. We are grateful to Kyowa Hakko Kirin for providing TPO, FP6, and G-CSF, and to Kyokuto Pharmaceutical Industrial for the nonserum medium used in the EB formation. We also thank S. Ichimura for hESC culture.

This work was supported in part by a Grant-in-aid from the Japan Society of Promotion of Sciences (KAKENHI nos. 17390274, 18013012, 19390258, and 20015010); Research on Pharmaceutical and Medical Safety, Health and Labor Sciences Research Grants from the Ministry of Health, Labor and Welfare of Japan (H16-Iyaku-32); grants from the Astellas Foundation for Research on Metabolic Disorders; the Uehara Memorial Foundation; and the Sagawa Foundation for Promotion of Cancer Research (S.C.); and the Project for Realization of Regenerative Medicine (S.O.).

Authorship

Contribution: Y.Y. and T.S. performed the experiments; K.H. designed the NBT-coated yeast cell-phagocytosis test; M.S.-Y., and K.K. assisted with interpretation of experiments and provided insightful comments; Y.Y. interpreted the data, made the figures, and wrote the paper; T.T., M.K., and S.O. advised on experimental design; S.C. provided critical reading of the paper; T.S. and S.C. designed the research.

Conflict-of-interest disclosure: The authors declare no competing financial interests.

Correspondence: Shigeru Chiba, Department of Clinical and Experimental Hematology, University of Tsukuba, 1-1-1 Tennodai, Tsukuba, Ibaraki, 305-8575, Japan; e-mail: schiba-tky@umin.net.

References

1. Kaufman DS, Hanson ET, Lewis RL, Auerbach R, Thomson JA. Hematopoietic colony-forming cells derived from human embryonic stem cells. Proc Natl Acad Sci U S A. 2001;98:10716-10721.
2. Nakano T, Kodama H, Honjo T. Generation of lymphohematopoietic cells from embryonic stem cells in culture. Science. 1994;265:1098-1101.
3. Vodyanik MA, Bork JA, Thomson JA, Slukvin II. Human embryonic stem cell-derived CD34+ cells: efficient production in the coculture with OP9 stromal cells and analysis of lymphohematopoietic potential. Blood. 2005;105:617-626.

4. Chadwick K, Wang L, Li L, et al. Cytokines and BMP-4 promote hematopoietic differentiation of human embryonic stem cells. Blood. 2003;102: 906-915.
5. Cerdan C, Rouleau A, Bhatia M. VEGF-A165 augments erythropoietic development from human embryonic stem cells. Blood. 2004;103: 2504-2512.
6. Wang L, Menendez P, Shojaei F, et al. Generation of hematopoietic repopulating cells from human embryonic stem cells independent of ectopic HOXB4 expression. J Exp Med. 2005;201:1603-1614.
7. Keller G, Kennedy M, Papayannopoulou T, Wiles MV. Hematopoietic commitment during embryonic stem cell differentiation in culture. Mol Cell Biol. 1993;13:473-486.
8. Wang L, Li L, Shojaei F, et al. Endothelial and hematopoietic cell fate of human embryonic stem cells originates from primitive endothelium with hemangioblastic properties. Immunity. 2004;21: 31-41.
9. Lu SJ, Feng Q, Caballero S, et al. Generation of functional hemangioblasts from human embryonic stem cells. Nat Methods. 2007;4:501-509.
10. Takayama N, Nishikii H, Usui J, et al. Generation of functional platelets from human embryonic stem cells in vitro via ES-sacs, VEGF-promoted structures that concentrate hematopoietic progenitors. Blood. 2008;111:5298-5306.
11. Hübel K, Carter RA, Liles WC, et al. Granulocyte transfusion therapy for infections in candidates and recipients of HPC transplantation: a comparative analysis of feasibility and outcome for community donors versus related donors. Transfusion. 2002;42:1414-1421.
12. Mousset S, Hermann S, Klein SA, et al. Prophylactic and interventional granulocyte transfusions in patients with haematological malignancies and life-threatening infections during neutropenia. Ann Hematol. 2005;84:734-741.
13. Price TH. Granulocyte transfusion: current status. Semin Hematol. 2007;44:15-23.
14. Bhatia M. Hematopoietic development from human embryonic stem cells. Hematology Am Soc Hematol Educ Program. 2007;2007:11-16.
15. Suemori H, Yasuchika K, Hasegawa K, Fujioka T, Tsuneyoshi N, Nakatsuji N. Efficient establishment of human embryonic stem cell lines and long-term maintenance with stable karyotype by enzymatic bulk passage. Biochem Biophys Res Commun. 2006;345:926-932.
16. Thomson JA, Itskovitz-Eldor J, Shapiro SS, et al. Embryonic stem cell lines derived from human blastocysts. Science. 1998;282:1145-1147.
17. Suzuki T, Yokoyama Y, Kumano K, et al. Highly efficient ex vivo expansion of human hematopoietic stem cells using Delta1-Fc chimeric protein. Stem Cells. 2006;24:2456-2465.
18. Yuo A, Kitagawa S, Okabe T, et al. Recombinant human granulocyte colony-stimulating factor repairs the abnormalities of neutrophils in patients with myelodysplastic syndromes and chronic myelogenous leukemia. Blood. 1987;70:404-411.
19. Kumano K, Chiba S, Shimizu K, et al. Notch1 inhibits differentiation of hematopoietic cells by sustaining GATA-2 expression. Blood. 2001;98:3283-3289.
20. Vowells SJ, Sekhsaria S, Malech HL, Shalit M, Fleisher TA. Flow cytometric analysis of the granulocyte respiratory burst: a comparison study of fluorescent probes. J Immunol Methods. 1995; 178:89-97.
21. Richardson MP, Ayliffe MJ, Helbert M, Davies EG. A simple flow cytometry assay using dihydrorhodamine for the measurement of the neutrophil respiratory burst in whole blood: comparison with the quantitative nitrobluetetrazolium test. J Immunol Methods. 1998;219:187-193.
22. Emmendörffer A, Hecht M, Lohmann-Matthes ML, Roesler J. A fast and easy method to determine the production of reactive oxygen intermediates by human and murine phagocytes using dihydrorhodamine 123. J Immunol Methods. 1990; 131:269-275.
23. Decleva E, Menegazzi R, Busetto S, Patriarca P, Dri P. Common methodology is inadequate for studies on the microbicidal activity of neutrophils. J Leukoc Biol. 2006;79:87-94.
24. Harvath L, Falk W, Leonard EJ. Rapid quantitation of neutrophil chemotaxis: use of a polyvinylpyrrolidone-free polycarbonate membrane in a multiwell assembly. J Immunol Methods. 1980;37: 39-45.
25. Rado TA, Bollekens J, St Laurent G, Parker L, Benz EJ Jr. Lactoferrin biosynthesis during granulocytopoiesis. Blood. 1984;64:1103-1109.
26. Rado TA, Wei XP, Benz EJ Jr. Isolation of lactoferrin cDNA from a human myeloid library and expression of mRNA during normal and leukemic myelopoiesis. Blood. 1987;70:989-993.
27. Cowland JB, Borregaard N. The individual regulation of granule protein mRNA levels during neutrophil maturation explains the heterogeneity of neutrophil granules. J Leukoc Biol. 1999;66:989-995.
28. van de Winkel JG, Anderson CL. Biology of human immunoglobulin G Fc receptors. J Leukoc Biol. 1991;49:511-524.
29. van Lochem EG, van der Velden VH, Wind HK, te Marvelde JG, Westerdaal NA, van Dongen JJ. Immunophenotypic differentiation patterns of normal hematopoiesis in human bone marrow: reference patterns for age-related changes and disease-induced shifts. Cytometry B Clin Cytom. 2004;60:1-13.
30. Ball ED, McDermott J, Griffin JD, Davey FR, Davis R, Bloomfield CD. Expression of the three myeloid cell-associated immunoglobulin G Fc receptors defined by murine monoclonal antibodies on normal bone marrow and acute leukemia cells. Blood. 1989;73:1951-1956.
31. Kerst JM, van de Winkel JG, Evans AH, et al. Granulocyte colony-stimulating factor induces hFc gamma RI (CD64 antigen)-positive neutrophils via an effect on myeloid precursor cells. Blood. 1993;81:1457-1464.
32. Kerst JM, de Haas M, van der Schoot CE, et al. Recombinant granulocyte colony-stimulating factor administration to healthy volunteers: induction of immunophenotypically and functionally altered neutrophils via an effect on myeloid progenitor cells. Blood. 1993;82:3265-3272.
33. Carulli G. Effects of recombinant human granulocyte colony-stimulating factor administration on neutrophil phenotype and functions. Haematologica. 1997;82:606-616.
34. van Raam BJ, Drewniak A, Groenewold V, van den Berg TK, Kuijpers TW. Granulocyte colony-stimulating factor delays neutrophil apoptosis by inhibition of calpains upstream of caspase-3. Blood. 2008;112:2046-2054.
35. Kerst JM, Slaper-Cortenbach IC, von dem Borne AE, van der Schoot CE, van Oers RH. Combined measurement of growth and differentiation in suspension cultures of purified human CD34-positive cells enables a detailed analysis of myelopoiesis. Exp Hematol. 1992;20:1188-1193.
36. Nakamae-Akahori M, Kato T, Masuda S, et al. Enhanced neutrophil motility by granulocyte colony-stimulating factor: the role of extracellular signal-regulated kinase and phosphatidylinositol 3-kinase. Immunology. 2006;119:393-403.
37. Azzarà A, Carulli G, Rizzuti-Gullaci A, Minnucci S, Capochiani E, Ambrogi F. Motility of rhG-CSF-induced neutrophils in patients undergoing chemotherapy: evidence for inhibition detected by image analysis. Br J Haematol. 1996;92:161-168.
38. Ribeiro D, Veldwijk MR, Benner A, et al. Differences in functional activity and antigen expression of granulocytes primed in vivo with filgrastim, lenograstim, or pegfilgrastim. Transfusion. 2007; 47:969-980.
39. Hiroyama T, Miharada K, Sudo K, Danjo I, Aoki N, Nakamura Y. Establishment of mouse embryonic stem cell-derived erythroid progenitor cell lines able to produce functional red blood cells. PLoS ONE. 2008;3:e1544.
40. Nakahara M, Matsuyama S, Saeki K, et al. A feeder-free hematopoietic differentiation system with generation of functional neutrophils from feeder- and cytokine-free primate embryonic stem cells. Cloning Stem Cells. 2008;10:341-354.

Cancer Informatics

Libertas Academica

OPEN ACCESS
Full open access to this and thousands of other papers at http://www.la-press.com.

ORIGINAL RESEARCH

Robust Model Selection for Classification of Microarrays

Ikumi Suzuki[1], Takashi Takenouchi[1], Miki Ohira[2], Shigeyuki Oba[3,4] and Shin Ishii[1,3]

[1]Graduate School of Information Science, Nara Institute of Science and Technology, Takayama, Ikoma, Nara 630-0192, Japan. [2]Division of Biochemistry, Chiba Cancer Center Research Institute, Chiba 260-8717, Japan. [3]Graduate School of Informatics, Kyoto University, Gokasho, Uji, Kyoto 611-0011, Japan. [4]PRESTO, Japan Science and Technology Corporation.

Abstract: Recently, microarray-based cancer diagnosis systems have been increasingly investigated. However, cost reduction and reliability assurance of such diagnosis systems are still remaing problems in real clinical scenes. To reduce the cost, we need a supervised classifier involving the smallest number of genes, as long as the classifier is sufficiently reliable. To achieve a reliable classifier, we should assess candidate classifiers and select the best one. In the selection process of the best classifier, however, the assessment criterion must involve large variance because of limited number of samples and non-negligible observation noise. Therefore, even if a classifier with a very small number of genes exhibited the smallest leave-one-out cross-validation (LOO) error rate, it would not necessarily be reliable because classifiers based on a small number of genes tend to show large variance. We propose a robust model selection criterion, the min-max criterion, based on a resampling bootstrap simulation to assess the variance of estimation of classification error rates. We applied our assessment framework to four published real gene expression datasets and one synthetic dataset. We found that a state-of-the-art procedure, weighted voting classifiers with LOO criterion, had a non-negligible risk of selecting extremely poor classifiers and, on the other hand, that the new min-max criterion could eliminate that risk. These finding suggests that our criterion presents a safer procedure to design a practical cancer diagnosis system.

Keywords: gene expression, cancer diagnosis, mini-chip microarrays, supervised analysis

Cancer Informatics 2009:7 141–157

This article is available from http://www.la-press.com.

1. Introduction

Microarray technology[1] has been applied to predict prognosis of cancer patients by comparing gene expression profiles in cancer tissue samples, and its predictive power has been demonstrated for many types of cancers.[2–5] The prognosis prediction systems based on microarrays have been expected to be new efficient bio-markers that enable personalized cancer medicine.[6] We consider, in this paper, two problems in expanding the use of microarray-based prediction systems in real clinical scenes, namely, observation cost and reliability.[7]

To reduce the observation cost without losing reliability, there have been several efforts to design diagnosis systems involving small numbers of specially selected genes. Recently, specialized diagnostic microarrays harboring small numbers of genes, to say tens or hundreds genes, are developed based on a supervised analysis with a dataset taken by a full microarray system involving thousands or tens of thousands of genes.[5,8,9] Measurement cost per patient becomes smaller by reducing the number of genes that is involved in such a system. If number of spots on a chip is fixed, more spots corresponding to a single gene can be included in a chip, which enables more reliable measurement by averaging multiple spots of same genes, and/or more efficient measurement by diagnosing multiple patients simultaneously in a single chip.[8] Manufacturing cost of a chip can be reduced by designing mini-chip harboring small number of spots.[5]

To achieve a reliable predictor, a well-known trade-off problem exists even if the above-mentioned issue of observation cost is omitted; we should select as large a number of informative genes and as small a number of non-informative genes as possible. We often need a certain number of genes to gain prediction accuracy, partly because multiple informative genes tend to provide different kinds of information which are complementary to each other for the prediction, and partly because, even when a set of multiple genes provides identical information, observation noise can be reduced by averaging them. On the other hand, since the prediction error increases when non-informative genes are included, we need to reduce the number of non-informative genes, putting the observation cost aside. These two demands are a trade-off because the process of determining whether each gene is informative or non-informative itself is not always reliable enough, due to non-negligible noise and a limited number of observations.

In summary, our goal can be stated as to achieve a reliable predictor based on as few genes as possible, which is accomplished in a supervised analysis with the following three processes:

- a gene selection process,
- a supervised learning process that constructs predictors based on a labeled set of expression data of the selected genes, and
- an assessment process for the constructed candidate predictors.

There have been many options proposed for the first two processes, and comparisons of their combinations were made from the viewpoint of prediction error rates on test datasets, namely generalization performances.[10,11] In the present study, we use the following two procedures that were applied in the previous study.[12]

- Weighted voting (WV) classifier[13] with gene selection based on absolute t-score (T-WV)
- Linear-kernel support vector machine (SVM)[14] with recursive elimination of genes that have the smallest contribution to current classification performance (R-SVM).[15]

These procedures construct multiple candidate predictors with various numbers of genes included in the predictors. Since their prediction performances for independent test datasets depend on the number of genes, their assessment is crucial.

In the assessment process, the prediction performance of each candidate predictor is estimated based on the training data, and good estimation is obtained by reducing the estimation bias and the variance. Since the true performance on independent data in the future is unknown, we should select the best predictor with less bias and smaller variance of the estimated performance. In general, the bias-variance trade-off problem is inherent to all statistical models used for prediction, especially in the classification framework.[16,17] For prognosis prediction by microarray, several past studies focused on reducing the estimation biases of the prediction error rates in determining the best model[18–20] because inclusion of biases could lead to over-estimation of